Nitrogen Economy Strategies Define Distinct Functional Groups of Genotypes in a Miscanthus sinensis Progeny

Shehyar Iqbal, Maryse Brancourt-hulmel, Marion Zapater

GCB Bioenergy

WILEY

Global Change Biology Bioenergy
BIOPRODUCTS FOR A SUSTAINABLE BIOECONOMY

RESEARCH ARTICLE OPEN ACCESS

Nitrogen Economy Strategies Define Distinct Functional Groups of Genotypes in a *Miscanthus sinensis* Progeny

Shehyar Iqbal | Maryse Brancourt-Hulmel | Marion Zapater

BioEcoAgro Joint Research Unit, INRAE, Univ de Liege, Univ Lille, Univ Picardie Jules Verne, Chaussée Brunehaut, Entrées-Mons, France

Correspondence: Maryse Brancourt-Hulmel (maryse.hulmel@inrae.fr)

Received: 7 July 2025 | **Revised:** 4 November 2025 | **Accepted:** 18 November 2025

Keywords: bioenergy | ecosystem services | functional groups | intra-specific variability | nitrogen economy | nitrogen fluxes | nitrogen recycling | nitrogen uptake | perennial crop

ABSTRACT

Understanding nitrogen-use strategies in *Miscanthus sinensis* is essential for optimizing biomass production while minimizing environmental impact, and providing sustainable bioenergy and ecosystem services. Nitrogen recycling in *M. sinensis* is known to be efficient, but the extent of intra-specific variability and its translation into distinct functional strategies remain unknown to date. Our objective was to assess the intergenotypic variation in nitrogen uptake and recycling and their relation to biomass yield in a diploid *M. sinensis* progeny. Endogenous remobilization fluxes were calculated for 80 genotypes from seasonal nitrogen dynamics under nitrogen deficient conditions, showing substantial intergenotypic variation, ranging from 0.2 to 85 kg N ha^{-1} in spring and 5 to 158 kg N ha^{-1} in autumn. Recycling efficiency, defined as the remobilized nitrogen relative to maximum nitrogen quantity, did not correlate with biomass yield, indicating that nitrogen recycling was independent of plant size. Exogenous nitrogen uptake varied widely (5–241 kg N ha^{-1}) and was strongly correlated with biomass yield ($r = 0.72$), making it the dominant factor influencing productivity, while principal component analysis highlighted the contribution of nitrogen recycling traits. Three functional groups emerged from hierarchical clustering on the principal components. The first group comprised nitrogen-acquisitive genotypes with high uptake and productivity, suitable for low-input bioenergy systems and potential ecosystem services like nitrate removal in water catchment areas. The second group followed a conservative strategy, with efficient belowground nitrogen storage and endogenous recycling, supporting resilience to environmental stress. The third group comprised nitrogen-deficient genotypes with low uptake, remobilization, and productivity. These findings demonstrate that substantial variation in nitrogen economy traits defined distinct functional groups in *M. sinensis*, providing a framework for breeding ideotypes that sustain biomass under nitrogen-limited conditions through enhanced uptake or remobilization, while delivering ecosystem services through contrasting remobilization strategies that can support nutrient retention, soil nitrogen conservation, and water quality regulation.

1 | Introduction

The concept of ecosystem services arises from the observation that by degrading ecosystems, societies compromise their own well-being by losing the benefits provided by nature (Barnaud and Muradian 2024). A crop like miscanthus can play a role in such a context, as Tavakoli-Hashjini et al. (2020) identified it as a multifunctional crop providing provisioning services (energy), supporting services (soil formation, nutrient cycling, water holding capacity, and biodiversity), regulating services (climate regulation, water regulation, pollination), and cultural and socio-economic services. In particular, the water regulation service is of special interest in water catchment areas to maintain the quality of drinking water. For instance, Weik et al. (2022)

have proposed the cultivation of miscanthus in water catchment areas in some German regions as a contribution to mitigating the negative impacts of increasing nitrate levels in the soil. Such ecosystem benefits are further supported by miscanthus's ability to reduce nitrate leaching (Cibin et al. 2016; Ferrarini et al. 2017), manage inorganic and organic contaminated land, and restore ecosystem services (Nsanganwimana et al. 2014).

In this context, the cultivation of miscanthus, based on the interspecific hybrid *Miscanthus* × *giganteus*, is interesting, as this rhizomatous perennial grass is highly productive and can remobilize nitrogen (N) from aboveground to belowground organs in autumn so that the stems harvested in winter have a low mineral nutrient quantity (Beale and Long 1997; Strullu et al. 2011; Magenau et al. 2022). The nitrogen stored in the rhizomes is then available for the following year of growth thanks to its remobilization during spring regrowth, which reduces the need for exogenous nitrogen inputs (Strullu et al. 2011). These two processes are known as autumn and spring remobilization, respectively. Harvest can be carried out every year, mainly at the end of winter, when the stems are senescent, to maintain the sustainability of the crop, as early harvesting depletes belowground nitrogen stocks and therefore increases the need for exogenous nitrogen inputs (Strullu et al. 2011). In addition to high amounts of biomass, it has several environmentally favorable traits, such as low nitrate losses (Lesur et al. 2014), high water-use efficiency (Ferchaud and Mary 2016), and low nitrogen input needs as defined by its critical nitrogen dilution curve (Zapater et al. 2017). In their review, Cadoux et al. (2012) link these low requirements to (1) high nutrient uptake, (2) high absorbed nutrient efficiency, (3) significant spring nutrient remobilization, (4) efficient autumn nutrient remobilization, which is an important trait linked to the perennial nature of the crop, and lastly (5) a potential contribution of nitrogen fixation by bacteria. Moreover, it has demonstrated potential for phytostabilization on trace element-contaminated soils (Nsanganwimana et al. 2021).

Despite these favorable characteristics, a single sterile triploid clone of *Miscanthus* × *giganteus* (Greef et al. 1997; Głowacka et al. 2015) is currently grown commercially for biomass production (Ben Fradj et al. 2020; Kumari et al. 2024), which is risky in the case of new environmental pressures (climate, pathogens) and is even more serious as it is a perennial crop. *Miscanthus sinensis* is targeted for the development of new varieties because it can offer good performance in terms of biomass production (Arnoult and Brancourt-Hulmel 2015) and a composition suitable for new markets (Belmokhtar et al. 2017; Codina Gironès et al. 2017). It also shows good tolerance to frost (Farrell et al. 2006; Zub et al. 2012), water deficit conditions, including drought (van der Weijde et al. 2017; Nie et al. 2017; Stavridou et al. 2019; Weng et al. 2022), and flooding stress (De Vega et al. 2021), as well as salt stress (Chen et al. 2017; van der Cruijsen et al. 2024). In addition, it also has good capacity for carbon sequestration (Briones et al. 2023) and phytoremediation (Zheng et al. 2022). It exhibits high intra-specific genetic variability (Sun et al. 2010; Zhao et al. 2013), which could help secure and expand the production area while maintaining decent yields. Like *M.* × *giganteus*, *M. sinensis* also exhibits nitrogen recycling capacities by efficiently remobilizing nitrogen during spring and autumn (Leroy et al. 2022), allowing nutrient-depleted stems at harvest and supporting growth under nitrogen-poor conditions (Lewin et al. 2024).

However, while the existence of nitrogen recycling in *M. sinensis* is established, the extent of its variability within the species remains poorly documented. Leroy et al. (2022) report variability in nitrogen recycling between two *M. sinensis* genotypes, suggesting that such variability may be widespread. Yet, beyond these isolated comparisons, no systematic evaluation has been carried out to characterize intra-specific diversity in nitrogen recycling. Whether this diversity leads to distinct nitrogen-use or nitrogen-economy strategies within *M. sinensis* is still an open question. Functional groups are often used to classify genotypes based on shared physiological traits, enabling researchers to identify plant types with distinct resource-use patterns (Byun et al. 2013; Fry et al. 2014). Yet, no such studies have been conducted to date for nitrogen-economy-related traits in *M. sinensis*, underlining the need to better understand how this variability may translate into functional differences among genotypes.

This study aimed to evaluate the intergenotypic diversity in nitrogen economy in a progeny of *M. sinensis* through the ability to reuse nitrogen stored in belowground parts. We hypothesized that the progeny would exhibit substantial functional diversity among genotypes, with variability across nitrogen-economy-related traits. Leroy et al. (2022) observed notable differences in nitrogen recycling between two genotypes, suggesting broader variability within the species. Analyzing variation between two parental cultivars and their progeny therefore provides a valuable framework to begin addressing this gap, while also laying the groundwork for broader studies across more genetically diverse accessions. Furthermore, we hypothesized that this diversity would follow structured patterns, leading to the formation of distinct functional groups. Rather than displaying a continuous gradient of nitrogen economy or nitrogen-use-related traits, the *M. sinensis* progeny may segregate into groups where some genotypes rely predominantly on nitrogen remobilization while others depend more on continuous uptake. To our knowledge, this is the first study to evaluate intra-specific variability in nitrogen economy in *M. sinensis* at the progeny scale, addressing a critical gap in understanding the species' nitrogen-use strategies. Furthermore, it pioneers the use of hierarchical clustering on principal components to identify distinct functional groups, providing new insights into how genotypic diversity shapes nitrogen-use strategies with direct implications for breeding and ecosystem service applications.

2 | Materials and Methods

2.1 | Experimental Site and Trial Design

The field experiment was conducted at the French National Research Institute for Agriculture, Food, and Environment (INRAE) in Estrées-Mons, northern France (49°87′ N, 3°01′ E). The site belonged to the UE GCIE, Unité Expérimentale Grandes Cultures Innovation Environnement (doi: 10.15454/1.5572425838988464E12). Regarding climatic data, the site experienced a marine west coast climate (Cfb). Over the last 8 years (2017–2024), the experimental site was characterized by a mean annual temperature of 11.2°C and an average annual

precipitation of 675 mm. During the growing season of the study (February 2023 to February 2024), the mean temperature was 11.4°C, and the mean precipitation was 925 mm.

The study was carried out over the 2023–2024 growing season and included two complementary field trials: the progeny trial and the parental trial. The progeny trial comprised 127 *Miscanthus sinensis* genotypes derived from a diploid cross between *M. sinensis* 'Malepartus' (MAL) and 'Herman Mussel' (HER). Seeds resulting from the cross were germinated in vitro in 2014. The resulting seedlings were planted in a greenhouse in 2015 and then transferred to Orléans in 2016, where the plants were clonally propagated by dividing rhizomes in 2017. The trial at Estrées-Mons was established in 2018 using an incomplete block design with four blocks and a planting density of 1 plant m^{-2}. A subset of 80 genotypes was selected for detailed analysis of nitrogen uptake and remobilization. Each genotype was represented by at least one replicate in each block. The parental trial, established with the two parental genotypes (MAL and HER), included increased replications with 15 plants per genotype at each sampling date (60 replications per genotype per season) and extended sampling over two growing seasons (2023–2024 and 2024–2025) to support the characterization of nitrogen status in the progeny trial. In the progeny trial, plant emergence occurred between March 24 and April 11, 2023. The duration of the growing season, defined as the time from emergence to complete senescence (95% of the aboveground part senesced by visual scoring) ranged from 201 to 270 days across genotypes. On average, 50% senescence was reached on Day of Year (DOY) 304, while 95% senescence occurred around DOY 333. Both the progeny and parental trials were unfertilized and irrigated throughout the 5 years of cultivation to ensure non-limiting water conditions. Recorded irrigation volumes for the years 2021 to 2023 amounted to 36, 926, and 393 m^3 in the progeny trial, and 140, 738, and 521 m^3 in the parental trial, respectively.

From establishment in 2018 until 2023, management primarily consisted of standard agronomic practices, including manual weed control, with no chemical inputs applied, and the plants were harvested each year in February. Leaf litter and other plant residues senesced naturally during autumn to winter and were left on the soil surface. During the 2023–2024 measurement cycle, however, fallen leaves from plants designated for the fourth (February 2024) sampling were systematically collected. Nets were installed over these plants throughout the senescence period, and leaves were gathered at regular intervals to quantify nitrogen losses through fallen leaves.

The soils at the Estrées-Mons site are deep silt loam, classified as Haplic Luvisols (IUSS Working Group WRB 2022). Soil texture was approximately 16.5% clay, 72.7% silt, and 7.8% fine sand, with a near-neutral pH (7.9), a high cation exchange capacity (96.8 meq 100 g^{-1}), and a moderate organic carbon content (11.4 g kg^{-1}; C/N = 10.6). These physicochemical characteristics were determined in 2017 and are considered representative of the site's baseline fertility. Soil mineral nitrogen concentrations were measured in both the progeny and parental trials over the 0–150 cm depth in early spring. In March 2023, the mean soil mineral N concentrations were 20 kg N ha^{-1} in the progeny trial and 13 kg N ha^{-1} in the parental trial. In March 2024, these values increased to 29 kg N ha^{-1} and 25 kg N ha^{-1}, respectively. These levels were markedly lower than those recorded in a previously studied, fertilized trial, located at the same site, in which 120 kg N ha^{-1} was applied as a urea-ammonium-nitrate solution in May. In which the soil mineral N concentrations measured in March or April over the 0–150 cm profile were 85, 85, 53, and 54 kg N ha^{-1} in 2014, 2015, 2016, and 2017, respectively (Leroy et al. 2022).

During each plant sampling campaign, soil N concentrations were also measured in the 0–30 cm horizon, where most root activity occurs. In the progeny trial, mean values were 8 kg N ha^{-1} in March 2023, 11 kg N ha^{-1} in July 2023, 12 kg N ha^{-1} in September 2023, and 19 kg N ha^{-1} in March 2024. In the parental trial, corresponding values were 5 kg N ha^{-1} in March 2023, 8 kg N ha^{-1} in August 2023, 10 kg N ha^{-1} in September 2023, 15 kg N ha^{-1} in March 2024, 16 kg N ha^{-1} in July 2024, and 15 kg N ha^{-1} in September 2024.

The nitrogen status of the progeny trial was assessed using the genotype *Miscanthus sinensis* 'Malepartus' (MAL), which served as a probe genotype. A probe genotype, as defined by Brancourt-Hulmel (1999), helps to diagnose nitrogen limitation through the nitrogen nutrition index (NNI) (Justes et al. 1994). MAL was chosen because it is one of the two parents of the progeny and, importantly, was present across all three reference trials: the unfertilized progeny trial, the unfertilized parental trial, and the historical fertilized trial (Leroy 2021). This allowed a direct comparison across nitrogen-limited and nitrogen-sufficient conditions, making it possible to diagnose the nitrogen status of the progeny trial.

The NNI was calculated as the ratio between the actual nitrogen concentration in the aboveground vegetative parts (N_a) and the critical nitrogen concentration (N_c), defined as the minimum concentration required to achieve maximum biomass production.

$$NNI = \frac{N_a}{N_c}$$

For *M. sinensis*, this critical nitrogen concentration was determined using the nitrogen dilution curve established by Zapater et al. (2017):

$$N_c = 23.4\, W^{-0.42} \text{ when } W > 1 \text{ t ha}^{-1}$$
$$\text{and } N_c = 23.4 \text{ when } W \leq 1 \text{ t ha}^{-1}$$

where W is the aboveground dry biomass (t ha^{-1}).

NNI was calculated with aboveground biomass and nitrogen concentration data for MAL, collected in July 2023 from the two previous trials represented by blue and red points, respectively, in Figure 1. These values were compared with historical data from 2016 and 2017 collected in the fertilized trial in July as well (Leroy 2021). In Figure 1, MAL data from the fertilized trial (green triangles) were positioned, as expected, close to or above the critical dilution curve, indicating nitrogen sufficiency or luxury status. In contrast, all MAL data points from the progeny and parental trials, both unfertilized, (red and blue) fell consistently below the curve, indicating nitrogen deficiency in both trials.

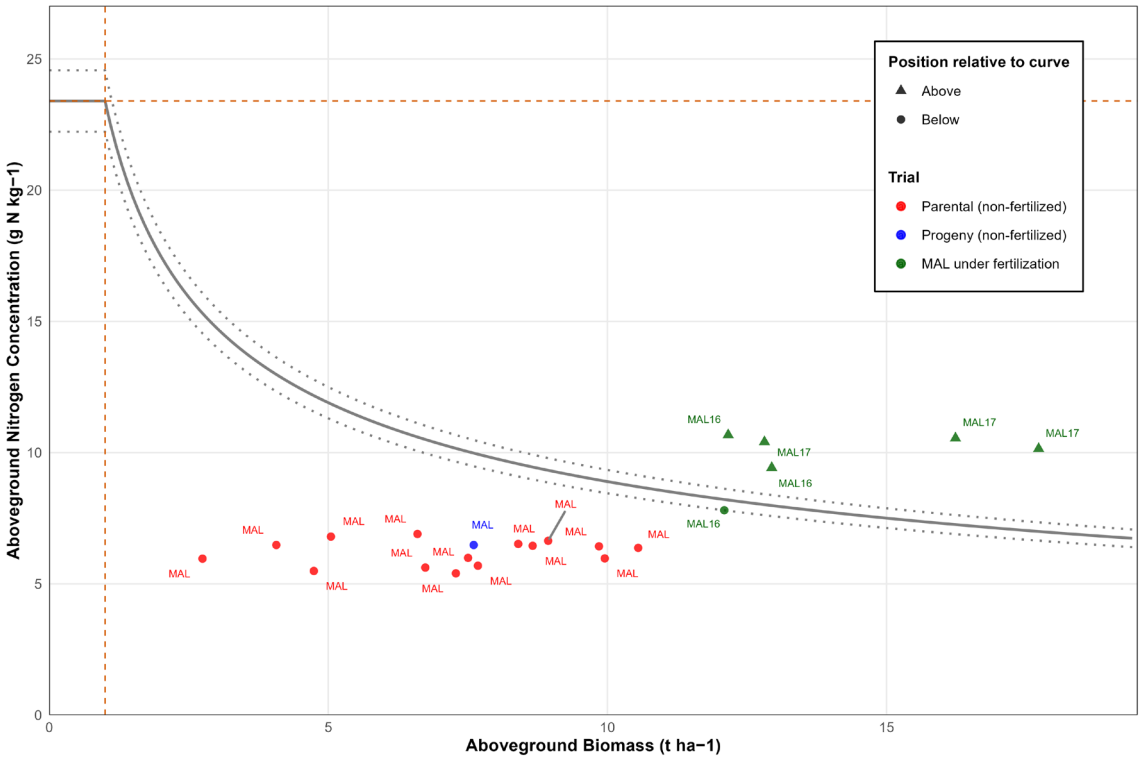

FIGURE 1 | Relationship between aboveground nitrogen concentration and aboveground biomass of *Miscanthus sinensis* (Malepartus), sampled across three field trials with contrasting soil nitrogen availability. Red and blue points represent samples from two non-fertilized trials (parental and progeny) collected in July 2023, while green points represent samples from a fertilized trial (120 kg N ha^{-1} applied as UAN) collected in 2016 and 2017. The black curve depicts the critical nitrogen dilution curve for *M. sinensis*, given by the equation: $Nc = 23.4 \times W^{-0.42}$ for $W > 1$ t ha^{-1}, $Nc = 23.4$ for $W \leq 1$ t ha^{-1} (Zapater et al. 2017), where Nc is the critical nitrogen concentration (g N kg^{-1}) and W is the aboveground biomass (t ha^{-1}). Dotted lines represent a ±5% confidence interval around the critical nitrogen dilution curve.

This diagnosis confirmed that the studied progeny trial was nitrogen-deficient for the probe genotype, suggesting that nitrogen availability may also be a limiting factor for other genotypes. NNI values calculated across the progeny population showed variation, with some genotypes classified as nitrogen-deficient and others as nitrogen-sufficient (data not shown).

2.2 | Plant Sampling

Plant sampling was carried out during four campaigns between February 2023 and February 2024 to assess nitrogen fluxes and remobilization dynamics in the *Miscanthus sinensis* progeny, following a refined protocol based on Leroy et al. (2022) (Figure 2). On each sampling date, both aboveground parts (AP: stems and leaves) and belowground parts (BP: rhizomes and associated roots) were collected to determine nitrogen quantities associated with specific stages of the plant's annual growth cycle. Rhizomes and associated roots were sampled to a maximum depth of approximately 30–40 cm, which corresponded to the maximum rhizome depth.

Each sampling date represented a key period in the annual cycle, characterized by distinct nitrogen stocks in the aboveground and belowground parts of the plants: February 2023 (dormancy, representing maximum nitrogen quantity in belowground parts), July 2023 (minimum nitrogen quantity in belowground parts), September 2023 (maximum nitrogen quantity in aboveground parts during active growth), and February 2024 (end of the growth cycle, when nitrogen had been remobilized to belowground parts for winter dormancy).

The samplings were conducted on 80 genotypes from the progeny trial, along with the two parental genotypes in the parental trial. Of the progeny genotypes, 65 had at least four replicates each, allowing one plant per genotype to be sampled on each of the four sampling dates. The remaining 15 genotypes had at least eight replicates each, which allowed two plants per genotype to be sampled per date, providing within-date replication for the analysis of variance.

2.3 | Plant Measurements and Determination of Biomass and Nitrogen Concentration

At each sampling date, the collected aboveground and belowground plant parts were used to assess biomass and nitrogen concentration. Aboveground plant parts were harvested at 7 cm above the soil surface, a commonly used cutting height in miscanthus plot trials (Cadoux et al. 2014; Scordia et al. 2022), consistent with standard mechanical harvesting practices. In our study, aboveground biomass included both the harvested part and the basal stems remaining below the cutting height, which were collected during rhizome excavation to ensure complete accounting of aboveground biomass and better reflect biomass and nitrogen dynamics. Belowground parts were excavated

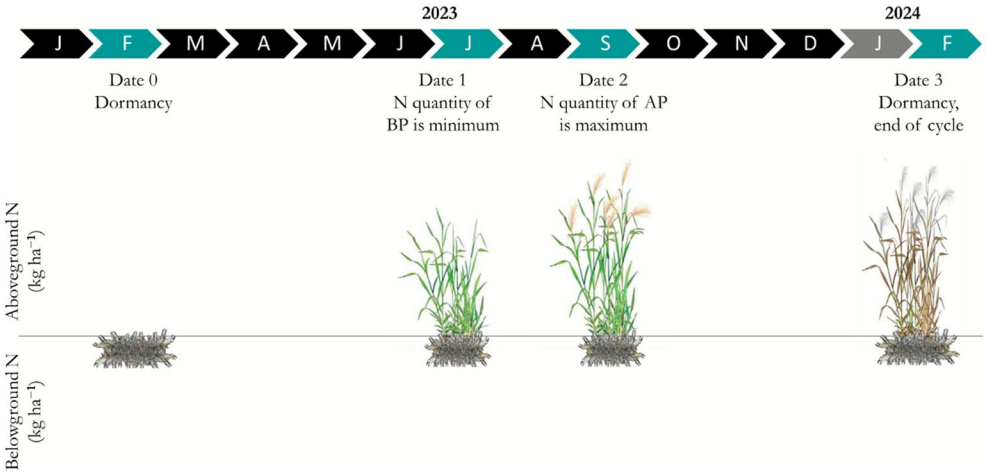

FIGURE 2 | Seasonal evolution of nitrogen stocks in the aboveground and belowground parts during key periods of nitrogen recycling over the course of 1 year (plant cycle). Adapted from Hou et al. (2022) and Leroy et al. (2022).

as described previously. The collected samples were weighed fresh, and a representative subsample was taken for dry matter determination. The subsample was weighed fresh, dried at 65°C for 96 h until a constant weight had been achieved, and then weighed again to determine dry weight. The dry matter content was calculated as:

$$\text{Dry Matter Content} = \text{Dry weight of subsample} / \text{Fresh weight of subsample}$$

This dry matter content was then used to estimate the dry biomass of the entire sample:

$$\text{Dry Biomass} = \text{Fresh Weight of Entire Plant} \times \text{Dry Matter Content}$$

Biomass yield ($t\,ha^{-1}$) was subsequently determined based on the dry biomass and the planting density.

Corrections of the raw biomass data were made to reduce potential bias due to a plant effect, as sampling belowground biomass is a destructive process. The same plants could not be reused on several sampling dates. As a result, a different plant for each genotype was sampled at each of the four time points, leading to plant-to-plant variability between the four plants sampled. This plant effect introduced potential bias in nitrogen flux calculations due to confounding between the nitrogen fluxes and the plant effect.

To mitigate this bias, the adjustment was based on aboveground biomass, given its strong and stable correlation with belowground biomass ($r = 0.85$ in February 2023; $r = 0.84$ in February 2024, Figure 3). The procedure followed four steps:

Step 1. Calculate the mean aboveground biomass of all plants per genotype sampled in the preceding years (February 2022 and February 2023).

Step 2. Determine the mean aboveground biomass of each individual plant across the two preceding years (February 2022 and February 2023).

Step 3. Compute a correction percentage for each plant:

$$\text{Correction Percentage} = (\text{Mean Biomass per Plant} / \text{Mean Biomass per Genotype}) \times 100$$

Step 4. Apply this correction percentage to both aboveground and belowground biomass values:

$$\text{Adjusted Value} = (\text{Raw Value} / \text{Correction Percentage}) \times 100$$

By applying this correction, the bias introduced by plant-to-plant variability was minimized, allowing for more reliable nitrogen flux calculations between sampling dates.

The nitrogen concentration of each sample was analyzed to quantify nitrogen fluxes and recycling rates across different growth stages.

The total nitrogen quantity of the plant was calculated as follows:

$$NA = WA \times [NA]$$
$$NB = WB \times [NB]$$
$$NT = NA + NB$$

where NA and NB represent the nitrogen quantity ($kg\,N\,ha^{-1}$) in aboveground and belowground compartments, respectively, WA and WB correspond to the dry matter quantity of each compartment ($t\,ha^{-1}$), and [NA] and [NB] are the corresponding nitrogen concentrations ($g\,N\,kg^{-1}$ DM).

2.4 | Quantification of Nitrogen Remobilization, Uptake, and Corresponding Use Efficiencies

Nitrogen-economy traits were evaluated, including nitrogen fluxes, uptake, and remobilizations, along with their corresponding efficiencies. Nitrogen remobilization was assessed separately for spring and autumn through two complementary approaches: spring and autumn remobilization.

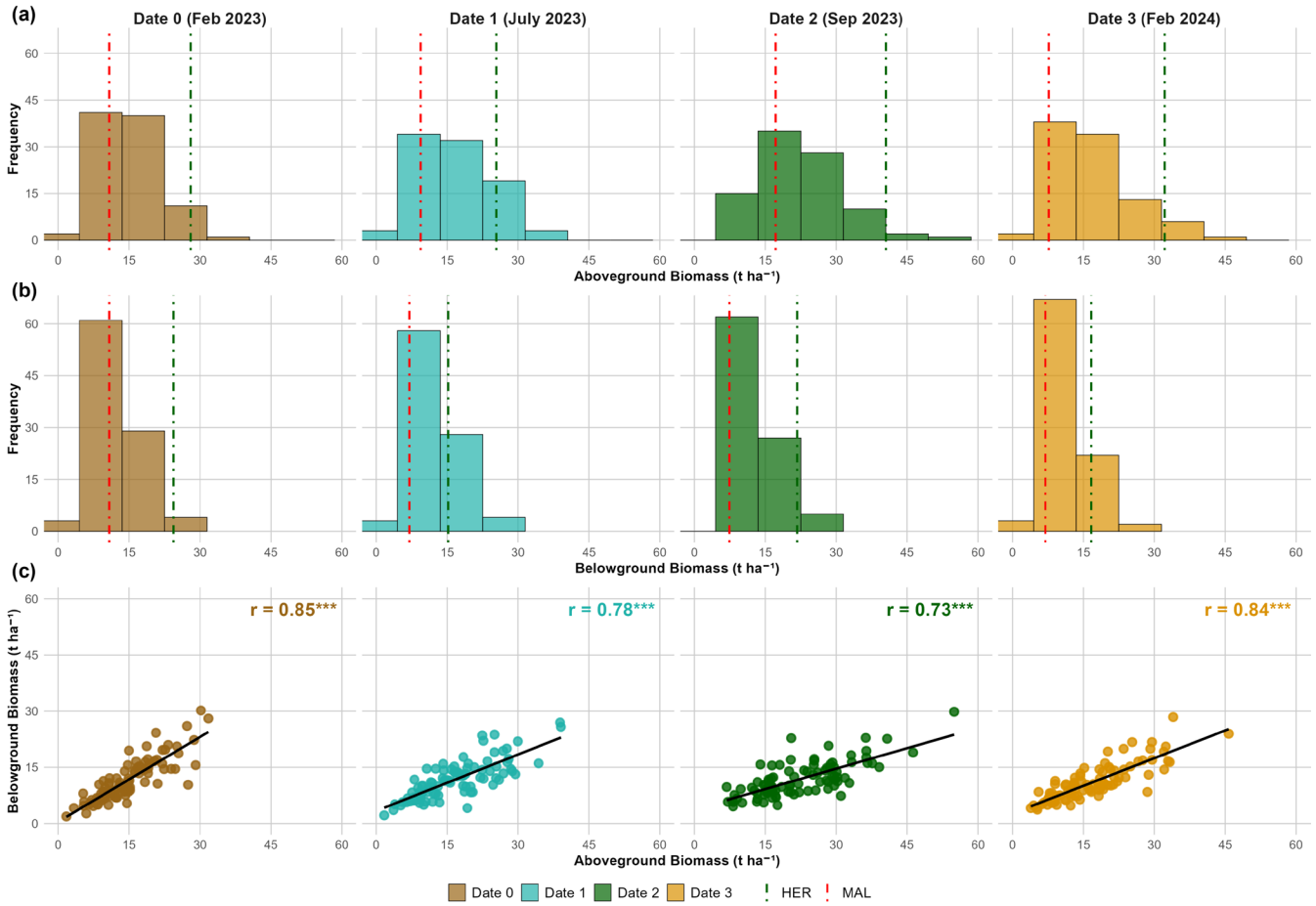

FIGURE 3 | Distribution of aboveground and belowground biomass (plots a and b) and their correlation (plot c) across four sampling dates during the 2023–2024 plant cycle. At Date 0, aboveground biomass belongs to the end of the previous plant cycle, whereas belowground biomass corresponds to both the end of the previous cycle and the beginning of the new one. The green and red dashed lines indicate the parental genotypes HER and MAL, respectively.

Spring remobilization (SR, kg N ha^{-1}), representing the nitrogen translocated from belowground storage organs to support new shoot growth in spring, was calculated following the method of Strullu et al. (2011) as:

$$SR = NB_0 - NB_1$$

where NB_0 was the nitrogen quantity in the belowground parts before spring regrowth (February 2023), and NB_1 was the nitrogen quantity after spring remobilization (July 2023), during summer.

The corresponding spring remobilization efficiency was calculated relative to maximum aboveground nitrogen quantity (NA_2):

$$SRE = \left(SR / NA_2\right) \times 100$$

Autumn remobilization (AR, kg N ha^{-1}), defined as the nitrogen withdrawn from senescing aboveground parts and stored in belowground organs before dormancy, was estimated using two methods described by Dierking et al. (2017): via aboveground method (ARa) and via belowground method (ARb).

$$ARa = NA_2 - NA_3$$

where NA_2 was the nitrogen quantity in aboveground parts at the start of senescence (September 2023), and NA_3 was the nitrogen quantity after full senescence (February 2024). ARa corresponds to the proportion of N in the aboveground part withdrawn during senescence.

$$ARb = NB_3 - NB_2$$

where NB_3 was the nitrogen quantity in belowground parts after full senescence (February 2024), and NB_2 was the nitrogen quantity in the belowground parts when aboveground nitrogen reached its maximum (September 2023). ARb corresponds to the proportion of N effectively withdrawn from the aboveground part that was finally stored in the rhizome.

As with spring remobilization efficiency, the corresponding autumn remobilization efficiencies were also calculated relative to maximum aboveground nitrogen quantity and were coded as ARaE and ARbE, respectively.

The nitrogen uptake (N Uptake, kg N ha^{-1}) represents the maximum nitrogen acquired from the soil during the growing season. It was calculated as:

$$N\ Uptake = NT_2 - NB_0$$

where NT_2 was the total nitrogen quantity of the whole plant at date 2 (September 2023), when aboveground biomass reached its peak nitrogen accumulation, and NB_0 was the nitrogen quantity in belowground parts before spring regrowth (February 2023). Similar to SRE, the corresponding nitrogen uptake efficiency was calculated relative to the maximum aboveground nitrogen quantity.

The nitrogen losses (N losses, kg N ha^{-1}) were calculated following the method of Leroy et al. (2022), considering the difference between total nitrogen at the peak of the growing season and after complete senescence:

$$\text{N losses} = NT_2 - NT_3$$

where NT_2 was the total nitrogen quantity at peak growth (September 2023), and NT_3 was the total nitrogen quantity at the end of the cycle (February 2024).

The nitrogen use efficiency (NUE, kg DM kg^{-1} N) represents the amount of biomass produced per unit of nitrogen accumulated in the plant. It can be calculated by considering the whole plant, but we chose to consider AP to be able to compare our results with other studies. Following the methodology of Ra et al. (2012); Olson et al. (2013) and Dierking et al. (2016) two NUE calculations were performed at different dates:

1. NUE_1: represents the plant's ability to produce aboveground biomass using nitrogen remobilized in spring and absorbed from the soil:

$$NUE_1 = WAmax / NA_2$$

where WAmax was the maximum biomass accumulated in the aboveground parts in September (t ha^{-1}), and NA_2 was the nitrogen quantity of the aboveground parts at date 2 (September 2023).

2. NUE_2: represents the amount of aboveground biomass that was harvested in February per Unit of Nitrogen Exported at the end of the growth cycle

$$NUE_2 = WA_3 / NA_3$$

where WA_3 was the aboveground biomass at date 3, and NA_3 was the nitrogen quantity of the aboveground parts at date 3 (February 2024).

In order to name all traits in a relevant manner, a *Miscanthus* ontology was developed at the INRAE BioEcoAgro research unit of Estrées-Mons (https://urgi.versailles.inra.fr/ephesis/ephesis/ontologyportal.do) by using the GnpIS multispecies integrative information system from the INRAE-URGI of Versailles (Steinbach et al. 2013). The data that support the findings of this study, along with variable names and alternative trait abbreviations, are openly available in *Recherche Data Gouv* at https://doi.org/10.57745/CEDLW2. (Iqbal et al. 2025).

2.5 | Statistical Analyses

All statistical analyses were conducted using R software (version 4.3.2, R Core Team). Data normality was assessed using the Shapiro–Wilk test, and homogeneity of variance was evaluated using Levene's test from the car package (version 3.1.3). When necessary, natural logarithm transformations were applied to nitrogen remobilization traits to meet the assumptions of normality and homoscedasticity required for analysis of variance (ANOVA).

The genotype effect on nitrogen remobilization fluxes, efficiencies, nitrogen uptake, and nitrogen use efficiency was analyzed using ANOVA, applied to the subset of the 15 repeated genotypes from the progeny trial. ANOVA models were fitted using the aov() function, and post hoc comparisons were conducted using the Least Significant Difference (LSD) test from the agricolae package (version 1.3.7). The overall threshold for statistical significance was set at $\alpha = 0.05$, with significance levels denoted as * $p < 0.05$, ** $p < 0.01$, *** $p < 0.001$, and NS for $p \geq 0.05$ in tables and figures. Pearson correlation analysis, based on the complete progeny subset of 80 genotypes, was used to assess pairwise relationships between nitrogen-economy traits and biomass yield.

To identify broader patterns in nitrogen-economy traits and classify genotypes with similar functional characteristics, hierarchical clustering on principal components (HCPC) was performed following the method of Husson et al. (2010). This involved conducting a principal component analysis (PCA) followed by hierarchical clustering using Ward's method with k-means consolidation. PCA was used to improve clustering reliability by retaining the essential variance while minimizing noise.

PCA was performed using the PCA() function from the FactoMineR package (version 2.11), with nitrogen remobilization fluxes including spring remobilization (SR), autumn remobilization via the aboveground method (ARa) and the belowground method (ARb), as well as nitrogen uptake and nitrogen losses, included as active variables. Biomass yields in September 2023 (Biomass S) and February 2024 (Biomass F) were included as quantitative supplementary variables. Nitrogen status, based on the nitrogen nutrition index, was included as a qualitative supplementary variable, distinguishing genotypes as either luxury or deficient.

Hierarchical clustering on all five principal components (explaining 100% of the variance) was performed using the HCPC() function in FactoMineR (version 2.11) to define functional groups of genotypes with similar nitrogen-economy characteristics. The statistical contribution of each variable to the formation of these groups was evaluated using v-test values.

In parallel, a second PCA was conducted using nitrogen remobilization efficiencies as active variables, followed by hierarchical clustering on the resulting principal components to evaluate the role of efficiency traits in shaping functional groupings.

3 | Results

The progeny exhibited great variability in biomass production in the above and belowground parts during the growing season.

Significant variability was observed in aboveground and belowground biomass of the *Miscanthus sinensis* progeny at the sampling dates during the 2023–2024 plant cycle (Figure 3a,b). Aboveground biomass ranged from 5 to 60 t ha^{-1}, with the highest values recorded in September. Belowground biomass showed a similar range, between 5 and 40 t ha^{-1}, with no seasonal trend. The parental genotypes HER and MAL, represented by the green and red dashed lines, respectively, were positioned at opposite ends of the distribution for multiple sampling dates, highlighting that the observed variability in the progeny reflects the genetic divergence between the parents (Figure 3a,b). We found a strong correlation between aboveground and belowground biomass at each sampling date in the progeny ($r = 0.85$, 0.78, 0.73, and 0.84 for Date 0, Date 1, Date 2, and Date 3, respectively), indicating that genotypes with high yield potential were also characterized by significant rhizome biomass (Figure 3c).

This observed variability highlighted the genetic diversity in biomass production potential among the progeny. As expected, we also found high variability in nitrogen quantities among the genotypes and across the dates (data not shown). This observed seasonality in nitrogen quantities provided key insights into nitrogen transfer and recycling within genotypes, serving as a basis for subsequent analysis of the nitrogen recycling variability in the progeny.

3.1 | Nitrogen Recycling, Assessed Through Remobilization Fluxes and Efficiencies in Autumn and Spring, Exhibited Substantial Variability Among the *M. sinensis* Progeny

Regarding spring remobilization fluxes, a huge variation was observed among the progeny, ranging from 0.2 to 85 kg N ha^{-1}, with parental genotypes MAL and HER showing fluxes of 22 kg N ha^{-1} and 10 kg N ha^{-1}, respectively (Figure 4a, Table 1). Spring remobilization efficiency (SRE), corresponding to the part of nitrogen in the aboveground part derived from spring remobilization, ranged from 0% to 80%, with parents MAL and HER at 27% and 3%, respectively (Figure 4b). Parental values fell within the broad progeny range, illustrating that variability extended beyond both parents. Differences between genotypes were substantial. The LSD values were 16.7 kg N ha^{-1} for SR and 21.1% for SRE (Figure 4), and when the difference between two genotypes exceeded these values, the genotypes were considered significantly different.

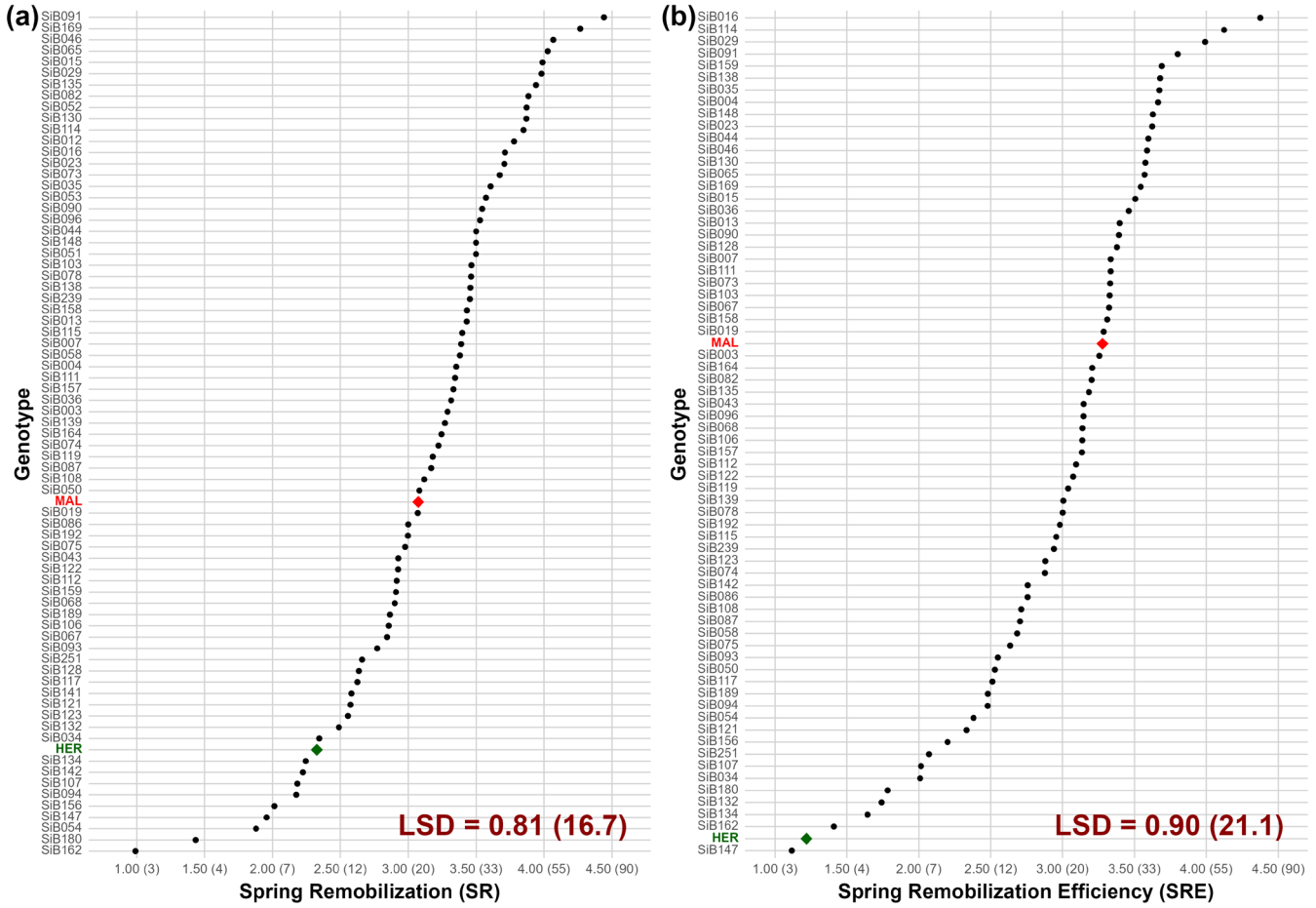

FIGURE 4 | Spring remobilization flux (SR) (plot a) and spring remobilization efficiency in proportion to maximum aboveground nitrogen (SRE) (plot b) across *Miscanthus sinensis* progeny. The *x*-axis scale shows log-transformed values. The corresponding non-transformed values are given in parentheses with units: Kg N ha^{-1} for (a) and % for (b). Each point represents the mean value. Green and red points highlight the HER and MAL genotypes, respectively. The least significant difference (LSD) is based on the subset of the 15 repeated genotypes to indicate the minimum difference required for statistical significance between genotypes.

TABLE 1 | Variables related to nitrogen recycling and nitrogen use efficiency in the progeny: Minimum, maximum, and mean values, as well as *F* values, *p* values, significance, and coefficient of variation (CV) of the ANOVA table. ANOVA results are based on the 15 repeated genotypes, and their corresponding minimum, maximum, and mean values are indicated in brackets.

Variable	Unit	Minimum	Maximum	Mean value	CV	*F*	*p*	Significance
Spring Remobilization (SR)	kg N ha^{-1}	0.2 (10.2)	84.9 (84.9)	27.0 (29.2)	37.5	8.46	7.8×10^{-8}	***
Autumn Remobilization (ARa)	kg N ha^{-1}	5.6 (26.2)	158.4 (137.1)	69.0 (76.2)	41.8	4.07	2.0×10^{-4}	***
Autumn Remobilization (ARb)	kg N ha^{-1}	0.5 (1.1)	72.8 (59.7)	28.6 (27.3)	56.1	3.30	2.1×10^{-3}	**
Nitrogen Uptake (U)	kg N ha^{-1}	5.2 (39.9)	241.2 (241.2)	93.9 (98.0)	30.2	13.8	1.3×10^{-11}	***
Spring Remobilization Efficiency (SRE)	%	0.2 (3.4)	79.5 (44.8)	23.5 (24.8)	53.0	2.03	4.2×10^{-2}	*
Autumn Remobilization Efficiency (ARaE)	%	7.0 (35.8)	86.3 (73.1)	54.7 (58.3)	20.5	2.56	9.5×10^{-3}	**
Autumn Remobilization Efficiency (ARbE)	%	0.6 (0.8)	65.4 (50.2)	26.2 (24.3)	62.4	3.54	1.2×10^{-3}	**
NUE_1	kg DM kg^{-1} N	122.7 (122.7)	365.3 (268.8)	195.1 (191.8)	15.5	5.02	1.6×10^{-5}	***
NUE_2	kg DM kg^{-1} N	161.7 (241.4)	553.2 (424.2)	328.4 (340.3)	10.2	9.84	2.8×10^{-9}	***

Note: Significance levels: ***$p<0.001$, **$p<0.01$, *$p<0.05$, NS $p\geq0.05$.

Concerning autumn remobilization, fluxes and efficiencies were expressed in terms of above and belowground parts. Fluxes calculated via aboveground (ARa) or belowground (ARb) methods ranged from 5 to 158 kg N ha^{-1} and 0 to 73 kg N ha^{-1}, respectively.

Mean value of autumn remobilization fluxes was significantly ($p<0.05$, data not shown) higher when calculated with the aboveground method (69 kg N ha^{-1}) than with the belowground method (28.6 kg N ha^{-1}) (Table 1), indicating that the quantity of nitrogen withdrawn from the aboveground part in autumn is bigger than the quantity of nitrogen stored in the rhizome in winter. Parental genotypes showed contrasting values, with MAL and HER at 63 kg N ha^{-1} and 114 kg N ha^{-1} for ARa, and 9 kg N ha^{-1} and 60 kg N ha^{-1} for ARb, respectively. Efficiencies, calculated as the proportion of nitrogen in the aboveground part withdrawn towards the rhizome (ARaE), or calculated as the proportion of N effectively withdrawn from the aboveground part that was finally stored in the rhizome (ARbE), also exhibited substantial variability among the progeny. ARaE ranged from 7% to 86%, with MAL and HER at 77% and 43%, respectively, while ARbE ranged from 1% to 65%, with MAL and HER at 11% and 26%, respectively. These parental positions represented different points within the progeny distributions, confirming that variation encompassed both parents (data not shown).

ANOVA based on the repeated genotypes confirmed significant genotype effects for all the preceding variables related to nitrogen recycling and nitrogen use efficiency (Table 1), further underlining the genotypic diversity in the progeny. The range of values for these repeated genotypes (in brackets in Table 1) covered quite well the range observed for the entire progeny. As expected, the coefficients of variation related to the fluxes or efficiencies were relatively high due to the involvement of several variables in their calculations. Nevertheless, highly significant effects were detected, highlighting significant genotype-dependent differences in nitrogen recycling behavior during the late growing season.

3.2 | Nitrogen Remobilization Fluxes Were Linked to Remobilization Efficiencies, but Not Between Seasons

Spring remobilization fluxes were strongly correlated with spring remobilization efficiency ($r=0.71$, Figure 5a).

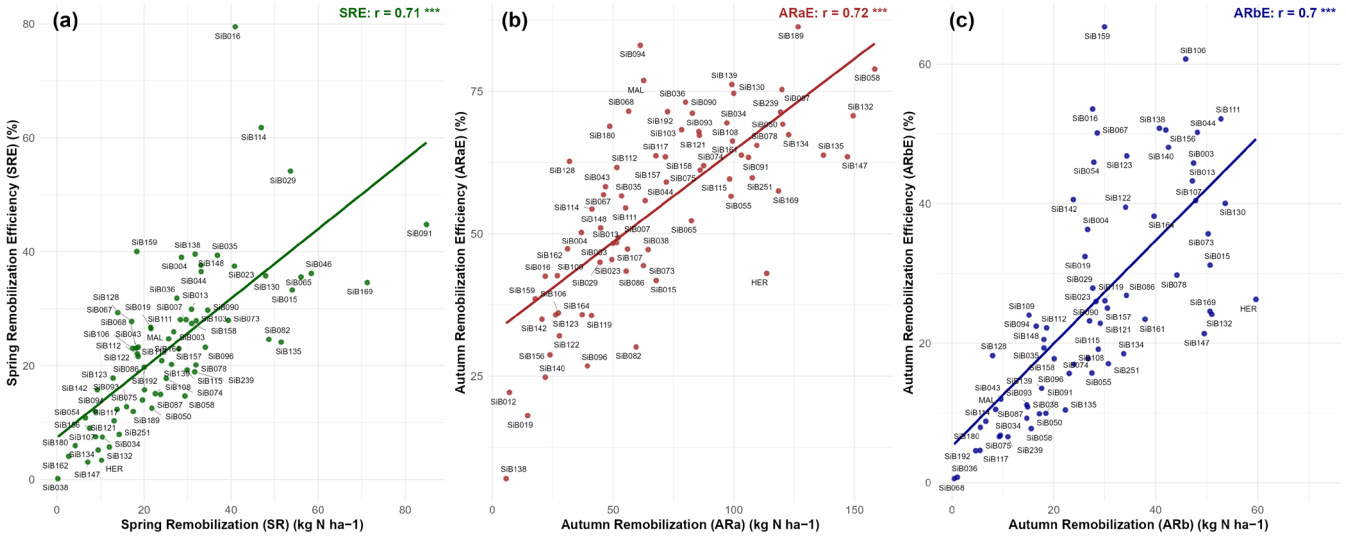

FIGURE 5 | Correlations in the progeny between spring remobilization, SR, autumn remobilization via aboveground method, ARa, and autumn remobilization via belowground method, ARb, respectively with their corresponding efficiencies SRE (plot a), ARaE (plot b) and ARbE (plot c). The Pearson correlation coefficient (r) is shown in the top right corner of each plot, along with its significance level. "***" indicates a highly significant correlation ($p < 0.001$).

Genotypes with higher nitrogen fluxes during the spring demonstrated greater remobilization efficiencies, indicating a consistent relationship between fluxes and efficiencies, which was partly expected given their mathematical dependence. In other words, a larger proportion of the nitrogen present in the aboveground part was derived from spring remobilization when the quantity of remobilized nitrogen in spring was higher.

Similarly, significant positive correlations were observed in autumn. Autumn remobilization fluxes significantly correlated with autumn remobilization efficiency using the aboveground and the belowground methods ($r = 0.72$ and 0.70, respectively, Figure 5b,c). Genotypes with higher nitrogen fluxes in autumn also exhibited greater remobilization efficiencies, whether we examined what was withdrawn from the aboveground part (Figure 5b) or what was finally stored in the belowground part (Figure 5c).

No significant correlations were found between spring and autumn remobilization fluxes (Figure 7). We observed a significant but weak relationship between spring and autumn remobilization efficiencies; however, this was considered to be non-relevant, as it was driven by only three genotypes that exhibited markedly different efficiencies compared to the other 77.

3.3 | Endogenous and Exogenous Nitrogen Strongly Influenced Biomass Production in *M. sinensis* Progeny

In perennial plants like miscanthus, the nitrogen accumulated by plants comes from both endogenous (reserve) and exogenous (soil) sources. Nitrogen Use Efficiency (NUE), representing the amount of biomass produced per unit of nitrogen accumulated in the plant, exhibited substantial variability among *M. sinensis* progeny. Throughout the growing season, the range of NUE progressively increased: from 111–195 in July 2023, to 123–365 in September 2023, and 162–553 kg DM kg^{-1} N in February 2024. This progressive increase indicated that nitrogen was utilized more efficiently as plants matured, particularly after the onset of senescence in February 2024.

NUE_1, corresponding to the plant's ability to produce aboveground biomass using both nitrogen remobilized in the spring (endogenous nitrogen) and nitrogen absorbed from the soil (exogenous nitrogen uptake), showed a weak but significant correlation with biomass yield in September 2023 and February 2024 ($r = 0.26$ and 0.23, respectively). To further examine how the two nitrogen sources influenced biomass, we investigated the respective effects of endogenous and exogenous nitrogen.

Regarding endogenous nitrogen, both spring and autumn nitrogen remobilization fluxes were positively correlated with biomass yield in February 2024 (brown harvest, Figure 6a, Table 1) as well as in September 2023 (green harvest, Figure 7). Spring remobilization fluxes showed a moderate correlation with biomass yield in September 2023 and February 2024 ($r = 0.34$ and 0.30, respectively). Stronger correlations were observed for autumn remobilization fluxes via aboveground method (ARa: $r = 0.62$ and 0.44, respectively) and via belowground method ($r = 0.31$ and 0.41, respectively), for the same dates (Figures 6a and 7). These results indicated that greater spring remobilization could contribute to increased aboveground biomass, although the moderate correlation suggested that other factors, such as exogenous nitrogen uptake, might also play a role. In turn, larger aboveground biomass in September appeared to support greater autumn remobilization, which contributed more strongly to the biomass yield observed in February.

In contrast, no significant correlations were observed between nitrogen remobilization efficiencies and biomass yield (Figures 6b and 7). In other words, biomass yield, whether at

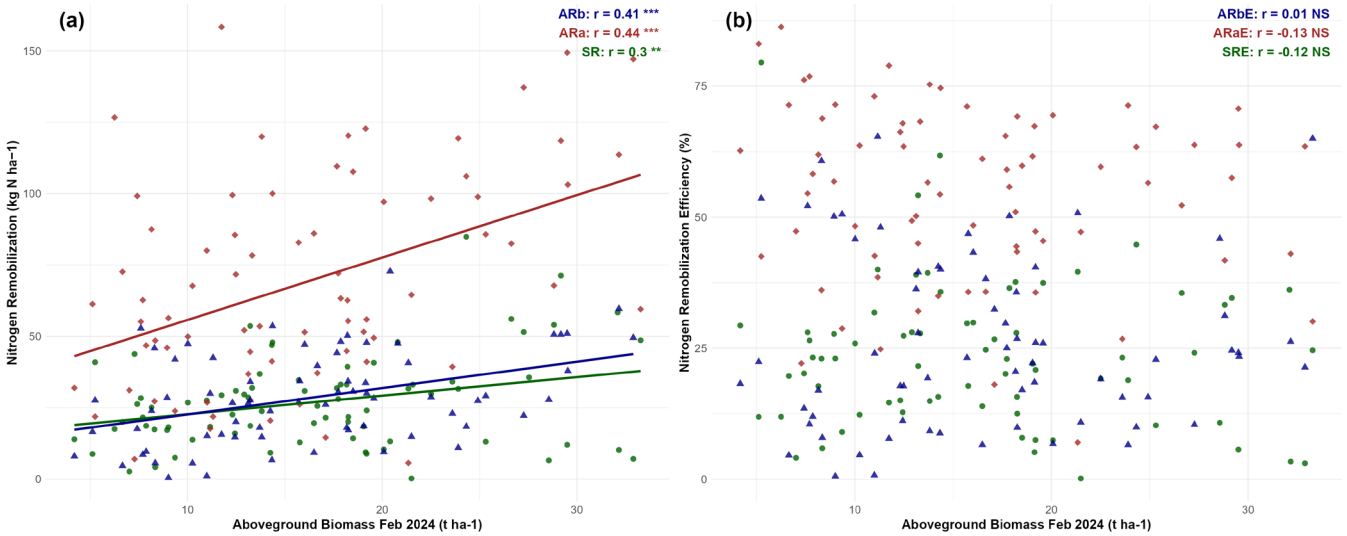

FIGURE 6 | Correlation between nitrogen remobilization fluxes (plot a) and nitrogen remobilization efficiencies (plot b) with biomass yield. The remobilization quantities are SR in green, ARa (AR calculated via aboveground method) in dark red, and ARb (AR calculated via belowground method) in blue, along with their respective efficiencies in proportion to maximum aboveground nitrogen. Pearson correlation coefficients (r) are shown, with *** for $p < 0.001$, ** for $p < 0.01$, and NS for non-significant correlations ($p \geq 0.05$).

the green or brown harvest, was not related to the proportion of nitrogen withdrawn from the aboveground part (ARaE), the proportion ultimately stored in the belowground part (ARbE), or the proportion of aboveground nitrogen derived from spring remobilization (SRE) (Figures 6b and 7). These findings suggested that plant functioning, in terms of nitrogen recycling, operated independently of biomass size across the progeny.

SRE and ARbE were significantly negatively correlated with nitrogen uptake ($r = -0.52$ and $r = -0.35$, respectively; Figure 7), indicating that genotypes with lower endogenous remobilization efficiency tended to rely more on exogenous nitrogen uptake.

Exogenous nitrogen uptake, corresponding to the quantity of nitrogen absorbed from the soil during the growing season, exhibited substantial variability among the *M. sinensis* progeny, ranging from 5 to 241 kg N ha^{-1}. The parental genotypes also differed, with MAL showing 56 kg N ha^{-1} and HER 241 kg N ha^{-1}, with HER positioned at the upper extreme of the progeny range. A significant positive correlation was observed between nitrogen uptake and aboveground biomass yield at both sampling dates ($r = 0.72$ and 0.63 in September 2023 and February 2024, respectively; Figure 7). Genotypes with higher nitrogen uptake produced greater biomass yields, demonstrating the strong link between nitrogen acquisition and productivity. This reciprocal relationship also reflected the influence of plant size on nitrogen uptake, with larger plants exhibiting greater uptake capacities.

However, nitrogen uptake efficiency, defined as the proportion of aboveground nitrogen derived from nitrogen uptake, was not significantly correlated with biomass yield in September 2023 ($r = 0.22$), and showed only a weak but significant correlation in February 2024 ($r = 0.24$; Figure 7). These results suggested that, while total nitrogen uptake was strongly linked to biomass accumulation, the efficiency with which absorbed nitrogen was converted into aboveground biomass was more variable and less predictive of yield.

Nitrogen uptake showed no significant correlation with spring remobilization fluxes (Figure 7). However, a strong positive correlation was observed between nitrogen uptake and autumn remobilization fluxes, particularly when calculated via the aboveground method ($r = 0.83$), while the belowground method showed no significant correlation (Figure 7). In other words, at the scale of the growing season, plants that absorbed more nitrogen (uptake) also withdrew greater amounts of nitrogen from the aboveground part. However, the result didn't highlight any relationship with the amount of nitrogen ultimately stored in the belowground part. This gap between the nitrogen withdrawn from the aboveground part and the amount finally stored in the belowground part was already highlighted by the comparison of the two methods used to calculate autumn remobilization, and indicated losses of nitrogen during the growing season.

Nitrogen losses were calculated as the difference between the total amount of nitrogen in the plant in September and in the following February, ranging from 2 to 143 kg N ha^{-1} across the progeny, with MAL and HER showing 54 and 71 kg N ha^{-1}, respectively. When expressed as a proportion of the total nitrogen quantity in the plant in September, these losses were highly variable, ranging from 2% to 67% (data not shown). These calculations did not take into account abscised fallen leaves prior to the final sampling date in February (Date 3). Between 1% and 27% of these nitrogen losses were accounted for by fallen leaves across the progeny. Nitrogen uptake was significantly correlated with nitrogen losses ($r = 0.70$, Figure 7), suggesting that genotypes absorbing higher amounts of nitrogen not only presented higher ARa (Figure 8) but also experienced greater nitrogen losses.

NUE_2 corresponded to the amount of biomass that could be harvested per unit of nitrogen exported at the end of the season (Date 3). It was significantly higher than NUE_1. This increase

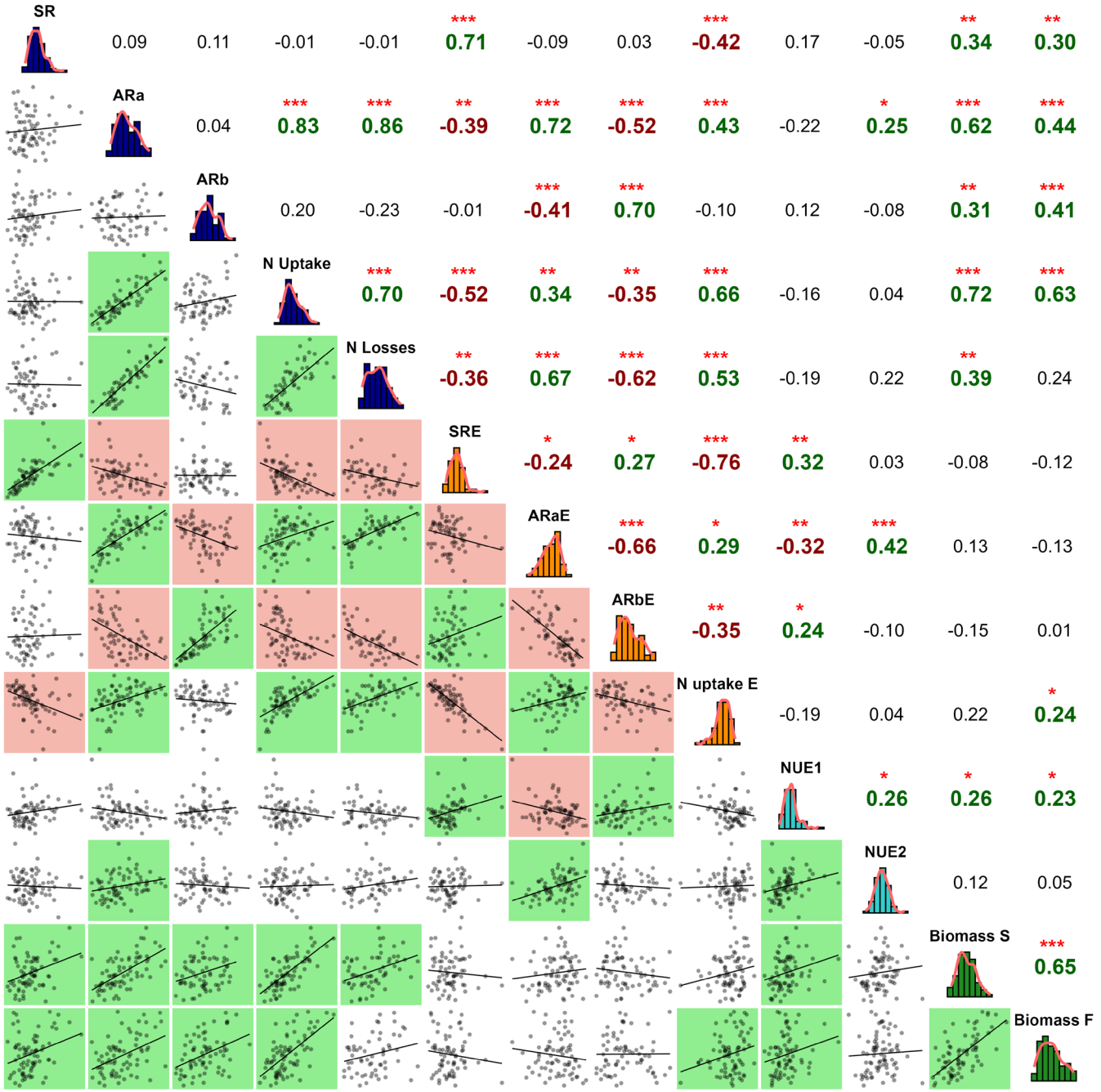

FIGURE 7 | Pairwise correlation matrix and scatterplots for nitrogen-related traits and aboveground biomass yield in *Miscanthus sinensis* progeny. Pearson correlation coefficients (r) are shown in the upper triangle, with significance levels indicated as follows: *** for $p < 0.001$, ** for $p < 0.01$, * for $p < 0.05$, and non-significant correlations ($p \geq 0.1$). Trait abbreviations are as follows: ARa, autumn remobilization flux calculated via aboveground method (kg N ha^{-1}); ARaE, autumn remobilization efficiency using the aboveground method (%); ARb, autumn remobilization flux calculated via belowground method (kg N ha^{-1}); ARbE, autumn remobilization efficiency using the belowground method (%); Biomass F, aboveground biomass in February 2024 (t ha^{-1}); Biomass S, aboveground biomass in September 2023 (t ha^{-1}); N Losses, nitrogen losses (kg N ha^{-1}); N uptake E, nitrogen uptake efficiency (%); N Uptake, nitrogen uptake (kg N ha^{-1}); NUE1, nitrogen use efficiency calculated in September 2023 (kg DM kg^{-1} N); NUE2, nitrogen use efficiency calculated in February 2024 (kg DM kg^{-1} N); SR, spring remobilization flux (kg N ha^{-1}); SRE, spring remobilization efficiency (%).

in NUE_2 was attributed to the seasonal decline in aboveground nitrogen quantity during autumn. Despite this higher efficiency, no significant correlations were observed between NUE_2 and biomass yield, either in September 2023 or February 2024 (Figure 7). These findings suggested that higher NUE_2 did not necessarily translate into greater biomass yield at the intergenotypic level, opening the way for further investigation into genotype classification through functional groups and the assessment of their distinct nitrogen utilization strategies.

Regarding the contribution of remobilization fluxes to nitrogen use efficiency, no significant correlations were observed between spring remobilization fluxes and NUE_1 (Figure 7). A weak positive correlation was found between autumn remobilization fluxes,

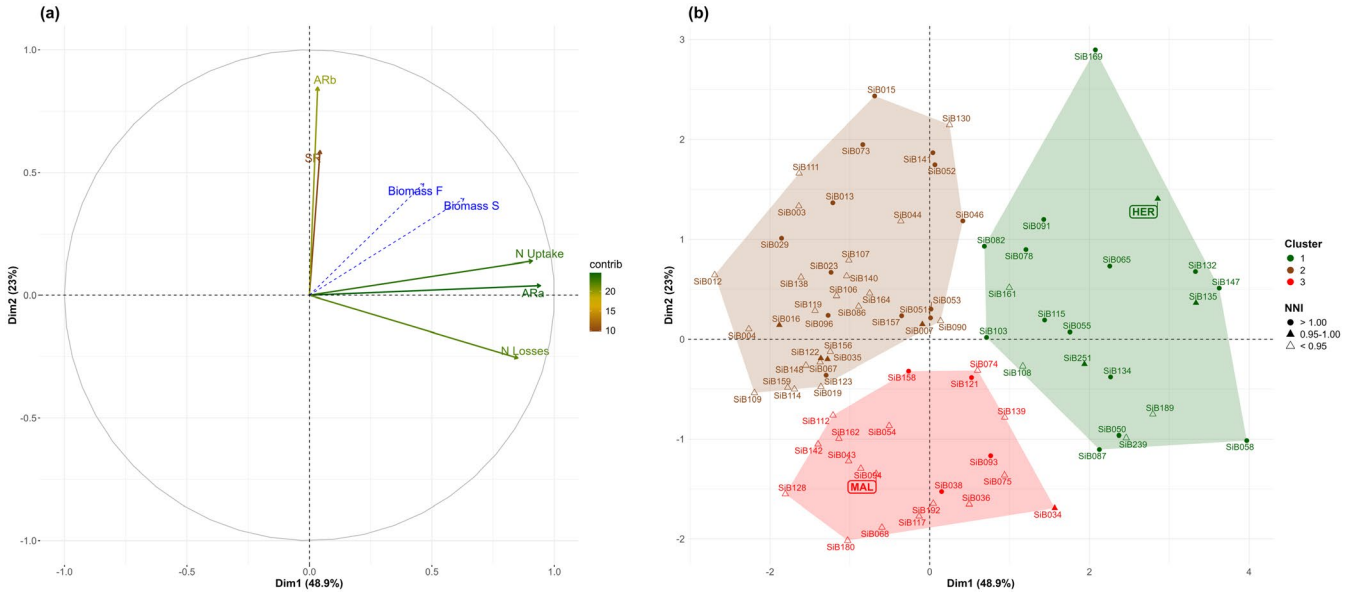

FIGURE 8 | Principal Component Analysis (PCA) and hierarchical clustering based on all five principal components. PCA biplot (plot a) and corresponding hierarchical clustering plot (plot b) of nitrogen remobilization fluxes, with biomass yield as a quantitative supplementary variable and nitrogen status as a qualitative supplementary variable. The variable coding is the same as in Figure 7.

calculated via the aboveground method, and NUE_2 ($r=0.25$), whereas no significant correlation was observed via the belowground method (Figure 7). These results suggested that plants that were more nitrogen-efficient, meaning those producing greater amounts of biomass per unit of nitrogen, tended to transfer larger quantities of nitrogen from the aboveground part toward the belowground part in autumn, even though the final amount of nitrogen stored in the rhizome was not significantly affected.

Significant correlations were found between spring remobilization efficiency and NUE_1 ($r=0.32$; Figure 7), indicating that nitrogen recycling during early growth stages contributed to improved nitrogen use efficiency. This suggested that nitrogen derived from spring remobilization formed an important part of the nitrogen sources building aboveground biomass.

In contrast, a significant negative correlation was observed between NUE_1 and autumn remobilization efficiency using the aboveground method (ARaE; $r=-0.32$), suggesting that plants with higher nitrogen use efficiency in September had less nitrogen remaining to be withdrawn from the aboveground part in autumn.

A significant positive correlation was also found between autumn remobilization efficiency (ARaE) and NUE_2 ($r=0.42$), whereas no such correlation was observed using the belowground method (Figure 7). These results indicated that plants producing more biomass per unit of nitrogen, whether remobilized or uptaken, also tended to remobilize nitrogen more efficiently in autumn.

3.4 | Genotypic Differences in Nitrogen Recycling and Uptake in the Progeny Led to the Formation of Functional Groups

The above results related to nitrogen remobilization, uptake, and use efficiency suggested that *M. sinensis* progeny did not follow a uniform nitrogen-use strategy. For example, higher NUE did not necessarily translate into greater biomass production at the intergenotypic level, supporting the existence of functional groups. To investigate these differences among genotypes, a multidimensional analysis was carried out through Principal Component Analysis (PCA), followed by a hierarchical clustering based on all five principal components (HCPC). Such an approach classified genotypes into distinct functional groups based on shared nitrogen economy characteristics.

A first PCA (Figure 8a) was performed using nitrogen remobilization fluxes as active variables. Biomass yield variables (Biomass F and Biomass S) were introduced as supplementary quantitative variables, and their position on the principal component axes allowed for the visualization of their relationship with the set of active nitrogen remobilization flux variables. Nitrogen status was introduced as a supplementary qualitative variable to describe the groups formed after clustering based on principal components. The genotypes were classified as nitrogen-deficient when their NNI was below 1 or nitrogen-sufficient when their NNI was above 1.

The first two principal components explained a substantial portion of the total variance (72%), with the first dimension of the PCA accounting for almost half (49%) and the second for a quarter (23%). The first component was associated with nitrogen uptake, nitrogen losses, and autumn remobilization via the aboveground method (ARa), representing aboveground nitrogen dynamics. The second component was linked to spring remobilization (SR) and autumn remobilization flux via the belowground method (ARb), reflecting belowground nitrogen recycling and early-season nitrogen remobilization processes.

Clustering based on the principal components (Figure 8b) grouped genotypes into three distinct groups (Clusters 1, 2, and 3 in Table 2). Of the 80 genotypes analyzed, Cluster 1 contained 21 genotypes (26%), Cluster 2 contained 38 genotypes (48%), and

TABLE 2 | Description of the three clusters based on the principal component analysis (PCA) and clustering of *Miscanthus sinensis* genotypes shown in Figure 8.

	Cluster 1		Cluster 2		Cluster 3	
	category	***v*.test**	**category**	***v*.test**	**category**	***v*.test**
Qualitative Variable	Luxury	3.17	Null		Deficient	2.39
Quantitative Variables	N. Uptake	6.69	ARb	3.76	Biomass F	−2.99
	ARa	6.66	SR	2.14	Biomass S	−3.69
	N. Losses	6.11	N. Uptake	−4.76	SR	−3.92
	Biomass S	5.36	ARa	−5.41	ARb	−5.16
	Biomass F	3.87	N. Losses	−5.57		

Note: The first line corresponds to the description of the clusters by the qualitative nitrogen status variable (deficient and luxury categories), with the value of the *v*-test corresponding to the magnitude of the variable category (deficient or luxury) involvement. In the second line, the most significant quantitative variables in the formation of each cluster are indicated by the *v*-test, where their signs correspond to positive or negative involvement and values describe their magnitudes; only the strongest (in absolute value) are shown. The coding of these quantitative variables is same as in Figure 7.

Cluster 3 contained 21 genotypes (26%). The supplementary variable about nitrogen status significantly influenced the formation of these three groups ($p = 0.001$; data not shown), highlighting the role of nitrogen availability in shaping genotypic behavior.

1. Cluster 1 consisted mainly of nitrogen-sufficient genotypes (71%), demonstrated higher nitrogen uptake, nitrogen losses, ARa, and biomass yield (Biomass F, Biomass S), reinforcing the positive influence of plant nitrogen status on productivity. This cluster represented high biomass-producing, nitrogen-sufficient genotypes and included 21 out of the 80 genotypes. The parental genotype HER was classified in this group, consistent with its high nitrogen uptake and sufficient nitrogen status (NNI = 0.97).
2. Cluster 2 was characterized by genotypes exhibiting lower nitrogen uptake, nitrogen losses, and ARa but higher belowground nitrogen recycling traits (ARb, SR). This group did not strongly associate with a clear nitrogen status. This cluster included genotypes that could be considered effective nitrogen storers and spring recyclers. It comprised 38 out of the 80 genotypes.
3. Cluster 3 primarily included nitrogen-deficient genotypes (81%), exhibited lower biomass production (Biomass F, Biomass S), lower ARb, and lower SR, reflecting the impact of limited nitrogen availability on these traits. This cluster represented low-biomass-producing, nitrogen-deficient genotypes and also included 21 out of the 80 genotypes. The parental genotype MAL was positioned in this group, reflecting its lower nitrogen uptake and deficient nitrogen status.

The contrasting placement of HER in cluster 1 and MAL in cluster 3 illustrated the divergence between the parents and showed how this divergence structured the functional groups identified in the progeny. Instead of the previously cited fluxes, a second PCA (data not shown) was conducted using nitrogen remobilization efficiencies as active variables, with biomass yield variables introduced as supplementary quantitative variables. The first principal component was primarily associated with nitrogen uptake efficiency and spring remobilization efficiency (SRE), while the second component was related to both spring and autumn remobilization efficiency, particularly ARaE.

However, clustering based on this PCA did not result in functionally distinct groups in relation to nitrogen recycling efficiencies, nitrogen status, or biomass production. In contrast to the first PCA, these results suggested that nitrogen recycling efficiency did not drive genotypic differentiation. Instead, nitrogen fluxes, nitrogen status, and uptake emerged as the dominant factors defining functional groups.

4 | Discussion

The results of this study provided clear evidence of substantial variability in the functioning of *M. sinensis* progeny in terms of nitrogen remobilization, uptake, and biomass production. Our first hypothesis proposed that genotypes would exhibit diverse functioning with significant differences in nitrogen recycling and acquisition traits. The second hypothesis predicted that this diversity would not follow a continuous gradient but instead would segregate into distinct functional groups based on shared nitrogen economy, i.e., endogenous and exogenous nitrogen fluxes and nitrogen use linked with biomass production. The discussion therefore focuses on three points: (1) the existence of genotypic diversity in nitrogen remobilization and uptake that highlights functional variability among the genotypes, (2) the existence of functional groups among genotypes regarding nitrogen recycling, and finally (3) the idea that spring remobilization efficiency reduces nitrogen uptake, while higher uptake enhances autumn remobilization and biomass yield.

4.1 | Genotypic Diversity in Nitrogen Remobilization and Uptake Highlights Functional Variability Among the Genotypes

Significant genotypic variation was observed across key nitrogen-related traits, including nitrogen remobilization fluxes,

efficiencies, and exogenous nitrogen uptake. These differences reflect not only genetic diversity but also functional variability, referring to differences in how genotypes acquire, recycle, and allocate nitrogen within the plant system. Together, these findings indicate that nitrogen acquisition and recycling were genotype-dependent, reflecting physiological flexibility and genetic control of nitrogen-economy traits within *M. sinensis* progeny.

The association between nitrogen remobilization fluxes and biomass production suggests that efficient endogenous recycling supported growth when exogenous nitrogen was scarce. Genotypes that remobilized larger nitrogen fluxes from storage organs during spring sustained greater aboveground biomass, indicating that remobilized nitrogen substituted for external inputs. Higher autumn remobilization fluxes were also positively correlated with aboveground biomass yield in February (Figure 7) and contributed to greater nitrogen transfer to belowground organs, enhancing nitrogen storage for the subsequent growth cycle. This aligns with findings in *Miscanthus* × *giganteus*, where delaying harvest until after senescence enables nitrogen translocation back to belowground storage organs, reducing external nitrogen requirements while maintaining long-term productivity (Strullu et al. 2011; Lewin et al. 2024). Recent multisite evidence in miscanthus also shows that spring harvest following full senescence is associated with lower tissue nitrogen contents across locations, consistent with nutrient relocation to rhizomes prior to harvest (Magenau et al. 2022). The observed variability in remobilization fluxes across genotypes further underscores the functional diversity in nitrogen allocation strategies within *M. sinensis*.

Nitrogen remobilization efficiencies in both spring and autumn also displayed substantial genotypic variability. Some genotypes were more efficient in recycling internal nitrogen than others, reflecting different physiological strategies for nitrogen use. Such differences may reflect genotypic variation in senescence timing, nitrogen transporter activity, and root–shoot nitrogen partitioning, which together determine how efficiently nitrogen is recycled within the plant.

Exogenous nitrogen uptake also varied considerably across genotypes. Some individuals absorbed more nitrogen from the soil, indicating variation in uptake capacity under low nitrogen conditions. While nitrogen availability in the trial was assumed to be uniform, minor spatial variability likely occurred due to soil heterogeneity and plant competition. Nonetheless, the observed differences suggest genotypic variation in nitrogen acquisition ability. Previous studies have shown that increasing nitrogen availability enhances biomass yield in *Miscanthus* × *giganteus*, although these findings are based on responses observed within a single genotype (Namoi et al. 2024). In the context of our study, we hypothesize that genotypes with low nitrogen uptake were unable to absorb sufficient nitrogen under the low nitrogen conditions of the trial. Their biomass production could therefore have increased if more nitrogen had been available.

The nitrogen status assessment based on Malepartus (Brancourt-Hulmel 1999; see Section 2) confirmed nitrogen-deficient conditions in the trial, which probably magnified differences among genotypes in their ability to compensate for limited soil nitrogen availability. Under such constraints, uptake capacity becomes a decisive component of the nitrogen economy, distinguishing genotypes able to sustain growth from those that rely primarily on remobilized reserves.

Taken together, these results confirm that *M. sinensis* progeny exhibit highly diverse nitrogen-economy traits, thereby validating our first hypothesis. The substantial variation in remobilization and uptake traits indicates that genotypic differences drive nitrogen-economy strategies, highlighting the potential for targeted breeding to optimize nitrogen efficiency in bioenergy crops. Breeding should prioritize genotypes that sustain high biomass and effective remobilization under limiting conditions, while assessing responsiveness under higher nitrogen to identify broadly adapted lines. Previous work indicates that nitrogen management can alter internal storage pools and recycling dynamics (Dierking et al. 2017). Integrating molecular and quantitative-genetic tools, including QTL mapping and genomic prediction (Atienza et al. 2003; Clark et al. 2019), will enable efficient identification of nitrogen-efficient ideotypes in *M. sinensis*.

4.2 | Genotypic Variation in Nitrogen Recycling Define Distinct Functional Groups in the Progeny

Three functional groups were identified through a hierarchical clustering on principal components, each group characterized by distinct nitrogen economy traits. Nitrogen status, used as a qualitative variable, significantly influenced the clustering, reinforcing the role of nitrogen availability in shaping genotypic behavior. Moreover, the clustering was structured primarily by nitrogen fluxes rather than remobilization efficiencies, highlighting that genotypic differentiation was driven by the net nitrogen movement rather than by the relative efficiency of recycling.

The first functional group (genotypes from Cluster 1) included nitrogen-sufficient genotypes that exhibited high nitrogen uptake, elevated nitrogen losses, and greater biomass yields, even under the nitrogen-limited conditions experienced in our experiment. These genotypes follow a nitrogen-acquisitive strategy, efficiently absorbing and utilizing available nitrogen to sustain growth and biomass production. Such a strategy, marked by rapid nitrogen uptake and high resource turnover, has also been documented in C_4 perennial bioenergy grasses, where it is considered an adaptive trait linked to productivity under variable environmental conditions (Heckman et al. 2024). Although the specific mechanisms were not analyzed in our study, this pattern may reflect greater root activity and transporter expression facilitating sustained nitrogen acquisition under low supply. Their ability to maintain high biomass productivity despite limited soil nitrogen availability suggests that they are well suited for low-input bioenergy systems. High nitrogen uptake capacity has been linked to improved biomass yield in resource-limited environments across perennial grasses (Namoi et al. 2024). Given these parallels, genotypes from this functional group hold potential for sustainable biomass production on degraded or marginal soils, where nitrogen fertilization is not viable or desirable.

The second functional group (genotypes from Cluster 2) was characterized by lower nitrogen uptake, reduced nitrogen losses, and lower aboveground remobilization (ARa) but higher belowground nitrogen recycling fluxes (ARb and SR). These genotypes can be described as effective nitrogen storers and spring recyclers, following a nitrogen-conservative strategy relying more on internal nitrogen recycling than external nitrogen acquisition. This strategy has been identified in perennial grasses and is typically associated with long-term resource conservation and reduced input dependency (Smith 2017). Unlike genotypes in other clusters, this group did not clearly align with nitrogen-deficient or nitrogen-sufficient status, indicating a more balanced or stable nitrogen-use pattern. The ability to store nitrogen efficiently in belowground organs may help these genotypes resume growth quickly after stress events such as late frost or drought. From an ecological standpoint, this behavior corresponds to a Root–Nitrogen–K-conservation (RNK) survival strategy, where plant success is linked to retaining critical resources during unfavorable periods (Chapin 1980). Similar nitrogen-conserving mechanisms have been reported in *Miscanthus* × *giganteus*. In a controlled study by Dierking et al. (2017), two *M.* × *giganteus* genotypes were compared under different nitrogen input levels, and under low nitrogen one genotype increased belowground nitrogen storage without sacrificing biomass yield, a conservative strategy relying on internal recycling rather than continuous external supply. This mirrors the functional characteristics observed in Cluster 2 genotypes of our study. Such traits may also contribute to ecosystem services by supporting long-term nitrogen retention in plant–soil systems, potentially stabilizing nutrient dynamics under low-input or variable environmental conditions.

Lastly, the third functional group (genotypes of Cluster 3) consisted primarily of nitrogen-deficient genotypes, with low nitrogen uptake and low remobilization fluxes, resulting in reduced biomass yield under nitrogen-limited conditions. While less productive, they may suit agroecosystems aiming to preserve soil nitrogen or reduce nutrient competition in mixed cropping. These genotypes may offer valuable traits, such as favorable biomass composition or morphology, making them useful in breeding. Crossing them with high-uptake genotypes might combine improved composition with stronger nutrient acquisition, though this requires experimental confirmation in breeding programs. Overall, they represent a complementary group for systems focused on nutrient stability or specific biomass goals rather than maximum yield.

These findings emphasize the functional diversity present within *M. sinensis* progeny and provide a framework for selecting genotypes tailored to different agroecological contexts. Since these groupings were derived under nitrogen-limited conditions, it remains essential to test their stability under higher nitrogen availability and across diverse environments. Future work should explore the physiological mechanisms behind the contrasting behaviors of Clusters 1 and 3, including root architecture, nitrogen transporter activity, and rhizosphere interactions, to determine how these traits influence acquisition and recycling under variable conditions. Understanding these mechanisms will enhance the targeted use of *M. sinensis* genotypes for both biomass production and ecosystem services.

These results confirm our second hypothesis, demonstrating that nitrogen-economy traits in *M. sinensis* are structured into distinct functional groups rather than distributed along a continuous gradient. This classification represents a novel approach in *Miscanthus* research, providing a functional framework for breeding nitrogen-efficient varieties.

4.3 | Endogenous Remobilization Efficiency Reduces Reliance on Nitrogen Uptake, While Higher Uptake Enhances Autumn Remobilization and Biomass Yield

Our study highlighted the central role of nitrogen uptake in driving biomass yield and shaping nitrogen remobilization dynamics in *Miscanthus sinensis*. Nitrogen uptake, defined as the nitrogen absorbed from external sources during the growing season, varied widely among genotypes (5–241 kg N ha^{-1}) and showed a strong positive correlation with aboveground biomass yield at both September 2023 and February 2024. This relationship underscores the reciprocal link between plant size and nitrogen uptake, whereby larger plants tend to absorb more nitrogen. However, nitrogen uptake efficiency did not correlate with biomass yield, suggesting that the quantity of nitrogen absorbed, rather than the efficiency of uptake, is the primary driver of biomass production.

In our unfertilized trial, the total aboveground nitrogen quantity measured in September was, on average, composed of 51% from nitrogen uptake, 16% from spring remobilization (SR), and 34% corresponded to other internal nitrogen pools. This distribution contrasts with findings from fertilized *Miscanthus sinensis* trials, where nitrogen uptake accounted for 75%–81% of total plant nitrogen, and spring remobilization contributed only 2%–11% in two genotypes (Leroy et al. 2022). The greater reliance on exogenous nitrogen uptake in fertilized systems highlights how nitrogen availability influences plant nitrogen sourcing strategies. In contrast, in our unfertilized system, the higher contribution of spring remobilization emphasizes the importance of internal nitrogen recycling in sustaining growth under low nitrogen conditions.

Interestingly, nitrogen uptake showed no correlation with spring remobilization fluxes (SR; $r = -0.01$), indicating that plants can have either high or low SR while still exhibiting a wide range of nitrogen uptake capacities. However, nitrogen uptake was significantly negatively correlated with spring remobilization efficiency ($r = -0.52$) and with autumn remobilization efficiency estimated via the belowground method ($r = -0.35$). These results indicate a compensatory trade-off, where genotypes with higher endogenous remobilization efficiency tend to depend less on exogenous nitrogen sources, while those with lower efficiency compensate through increased nitrogen uptake from the soil. To our knowledge, no such relationship has been documented in miscanthus until now, making these findings novel in the context of perennial bioenergy crops.

In contrast to spring remobilization, nitrogen uptake was positively correlated with autumn remobilization fluxes, particularly when calculated via aboveground method (ARa; $r = 0.83$). Higher nitrogen uptake increases the nitrogen reservoir available

for translocation during autumn senescence, a process crucial for storing nitrogen in rhizomes before winter. Autumn remobilization ensures the storage of nitrogen in rhizomes for use in the following growing season, linking current-season nitrogen uptake to long-term productivity (Muhammad et al. 2020). The strong correlation between nitrogen uptake and autumn remobilization underscores the importance of nitrogen uptake not only for current-season biomass production but also for sustaining perennial growth cycles. This relationship indicates that nitrogen acquired late in the growing season contributes to reserve formation in rhizomes, a process well documented in *M.* × *giganteus*, where decreases in shoot nitrogen during autumn coincide with increased rhizome nitrogen that supports regrowth in spring (Strullu et al. 2011; Dierking et al. 2017).

However, while nitrogen uptake and ARa were strongly correlated, no such relationship was observed between uptake and nitrogen ultimately stored belowground (ARb). This discrepancy suggests that not all nitrogen withdrawn from the aboveground parts during senescence was successfully transferred to rhizomes. Instead, part of this nitrogen was lost. It is also highlighted by our comparison of the two methods (ARa vs. ARb), which showed diverging values across genotypes. Nitrogen losses, calculated as the difference between total plant nitrogen in September and February, corresponded to 2%–67% of September nitrogen quantity. Of these losses, only a small fraction (1%–27%) was attributable to leaf abscission, indicating that a significant portion of nitrogen is lost through other physiological processes. Leroy et al. (2022) similarly reported winter nitrogen losses of 42%–56% in *M. sinensis*, of which only a small portion could be explained by fallen leaves. These findings highlight that nitrogen loss is a key yet understudied component of perennial nitrogen cycling.

Nitrogen losses beyond leaf abscission can be explained by several processes. Part of the nitrogen may be stored in deeper roots not captured by our sampling depth, although previous studies indicate that root nitrogen content decreases sharply with depth and is probably low (Neukirchen et al. 1999; Ferchaud et al. 2016). Other pathways include rhizodeposition and root turnover, which transfer organic and inorganic nitrogen from living roots to the soil, where it can be immobilized by microbes rather than recovered in rhizomes (Wichern et al. 2008; Heaton et al. 2010; Hromádko et al. 2010). Further losses may occur through gaseous emissions, including ammonia volatilization from aerial tissues (Schjoerring and Mattsson 2001) and nitrous oxide emissions directly mediated by plants (Pihlatie et al. 2005; Lenhart et al. 2019). The relative contribution of these processes remains uncertain in our trial, yet their combined effect offers a plausible explanation for the substantial nitrogen losses observed.

Together, these results revealed a dual nitrogen-use strategy among genotypes. Those with high nitrogen uptake achieved greater biomass and stronger autumn remobilization, supporting both immediate growth and nitrogen storage for the following season. In contrast, genotypes with high endogenous remobilization efficiency depended less on soil nitrogen, making them well-suited for low-input systems. This functional variation allows the selection of genotypes based on environmental objectives. High-efficiency, low-uptake genotypes may perform better in marginal soils with limited fertilizer availability, while high-uptake genotypes may be effective in nutrient-rich or polluted environments, such as water catchment areas or fields targeted for phytoremediation.

Since endogenous remobilization efficiencies are not correlated with biomass yield, genotypes can be selected for either high or low efficiency without sacrificing productivity. This reinforces the conclusion of the section: nitrogen uptake is the primary driver of both biomass yield and autumn remobilization, but high remobilization efficiency provides an additional pathway to reduce dependence on external nitrogen. Optimizing both traits in combination could enhance nitrogen-use resilience in *M. sinensis*, enabling sustained productivity and improved nutrient retention across contrasting agroecosystems.

5 | Conclusion

This study demonstrated substantial genotypic variability in nitrogen remobilization, uptake, and biomass production among *Miscanthus sinensis* progeny grown under nitrogen-deficient field conditions. Nitrogen economy traits, reflecting how plants acquire, redistribute, and use nitrogen, were shown to follow coherent, genotype-dependent strategies, each with distinct implications for productivity and nutrient cycling. The identification of functionally diverse genotypes provided valuable insights for optimizing *M. sinensis* for both bioenergy production and ecosystem services.

The results strongly supported our first hypothesis that *M. sinensis* progeny exhibited functional diversity in nitrogen remobilization and uptake. Spring and autumn nitrogen remobilization fluxes were strongly associated with biomass yield, reinforcing their role as an endogenous nitrogen source contributing to plant growth. However, nitrogen remobilization efficiencies were not correlated with biomass yield, indicating that genotypes with both high and low remobilization efficiencies could still achieve high biomass production. Genotypes with higher spring remobilization efficiency generally showed reduced reliance on nitrogen uptake, suggesting a trade-off between sourcing strategies. Conversely, high nitrogen uptake supported both greater autumn remobilization and biomass yield, making it a primary driver of productivity in low-input systems.

The study also addressed the second hypothesis by showing that *M. sinensis* genotypes grouped into three distinct functional groups, each defined by coherent nitrogen-economy traits: nitrogen-acquisitive genotypes can enhance yield in nutrient-limited systems; conservative types can improve nutrient retention in rotations; and low-uptake genotypes can preserve soil fertility in nitrogen-rich zones. These functional groupings, in particular the nitrogen-acquisitive and conservative types, provide a new framework for breeding nitrogen-efficient *M. sinensis* ideotypes, enabling genotype selection tailored to contrasting agroecosystem goals. Beyond breeding, these findings also hold broader significance for sustainable bioenergy cropping and ecosystem management.

Future studies should evaluate whether these functional groups remain stable across varying nitrogen availability, soil

conditions, and climatic regimes. Multi-environment trials, including contrasting management practices, will help identify genotypes that consistently maintain their nitrogen-acquisitive or conservative strategies across environmental gradients.

Investigating the physiological and molecular traits underpinning these groups, such as root architecture, microbial associations, and nitrogen transport mechanisms, will be key to refining selection criteria for nitrogen-efficient genotypes. From a genetic perspective, this study provides the physiological foundation for further quantitative-genetic dissection of nitrogen-related traits. The next step will be to estimate heritability and genetic correlations for remobilization, uptake, and efficiency traits, and to identify quantitative trait loci (QTLs) and genomic regions linked to nitrogen-economy mechanisms.

Expanding beyond the current parental backgrounds to a broader panel of genetically diverse *M. sinensis* accessions will further enhance understanding of the species' adaptive potential and improve the transferability of these findings to breeding programs across diverse agroecological zones. In summary, integrating multi-environment validation with ongoing QTL mapping and heritability analyses will help to transform this functional framework into a predictive, genetically informed breeding strategy for nitrogen-efficient, high-yielding *M. sinensis* cultivars.

Abbreviations

Genotypes, and Trials

Cfb	Marine west-coast climate
DOY	Day of Year
HER	*Miscanthus sinensis* 'Herman Mussel'
INRAE	French National Research Institute for Agriculture, Food and Environment
MAL	*Miscanthus sinensis* 'Malepartus'
UAN	Urea-ammonium-nitrate solution (applied at 120 kg N ha^{-1})
UE GCIE	Unité Expérimentale Grandes Cultures Innovation Environnement

Organs, Biomass, and Sampling Dates

AP	Aboveground parts (stems and leaves)
Biomass F	Aboveground biomass in February 2024 (t ha^{-1})
Biomass S	Aboveground biomass in September 2023 (t ha^{-1})
BP	Belowground parts (rhizomes and associated roots)
Date 0	February 2023 (dormancy; maximum N in BP)
Date 1	July 2023 (minimum nitrogen quantity in belowground parts)
Date 2	September 2023 (maximum nitrogen quantity in aboveground parts)
Date 3	February 2024 (after full senescence; harvest)
W	Aboveground dry biomass (t ha^{-1}) in the critical nitrogen dilution curve equation
WA	Biomass of aboveground parts (t ha^{-1})
WA_3	Aboveground biomass in February 2024 (t ha^{-1})
WAmax	Maximum aboveground biomass accumulated in September (t ha^{-1})
WB	Biomass of belowground parts (t ha^{-1})

Nitrogen Pools, Concentrations, and Quantities

N_a	Actual nitrogen concentration in aboveground vegetative parts (for NNI)
N_c	Critical nitrogen concentration from the critical nitrogen dilution curve
[NA]	Nitrogen concentration of aboveground parts (g N kg^{-1} DM)
[NB]	Nitrogen concentration of belowground parts (g N kg^{-1} DM)
N	Nitrogen
NA	Nitrogen quantity in aboveground parts (kg N ha^{-1})
NA_2	Nitrogen quantity of aboveground parts at Date 2 (September 2023)
NA_3	Nitrogen quantity of aboveground parts at Date 3 (February 2024)
NB	Nitrogen quantity in belowground parts (kg N ha^{-1})
NB_0	Nitrogen quantity in belowground parts before spring remobilization (February 2023)
NB_1	Nitrogen quantity in belowground parts after spring remobilization (July 2023)
NB_2	Nitrogen quantity in belowground parts when aboveground N is maximal (September 2023)
NB_3	Nitrogen quantity in belowground parts after full senescence (February 2024)
NNI	Nitrogen Nutrition Index ($=N_a/N_c$)
NT	Total nitrogen quantity in the whole plant (kg N ha^{-1})
NT_2	Total N quantity at peak growth (September 2023)
NT_3	Total N quantity at the end of the cycle (February 2024)

Nitrogen Fluxes and Efficiencies

ARa	Autumn remobilization via aboveground method (kg N ha^{-1}) = $NA_2 - NA_3$
ARaE	Autumn remobilization efficiency using the aboveground method (%)
ARb	Autumn remobilization via belowground method (kg N ha^{-1}) = $NB_3 - NB_2$
ARbE	Autumn remobilization efficiency using the belowground method (%)
N Losses	Nitrogen losses (kg N ha^{-1}) = $NT_2 - NT_3$
N uptake E	Nitrogen uptake efficiency (%), proportion of aboveground N derived from uptake
N Uptake	Nitrogen uptake (kg N ha^{-1}) = $NT_2 - NB_0$
NUE	Nitrogen use efficiency (kg DM kg^{-1} N)
NUE_1	$WAmax/NA_2$ (aboveground biomass produced using spring-remobilized and absorbed N)
NUE_2	WA_3/NA_3 (aboveground biomass harvested per unit of N exported at end of cycle)
SR	Spring remobilization (kg N ha^{-1}) = $NB_0 - NB_1$
SRE	Spring remobilization efficiency (%) = $(SR/NA_2) \times 100$

Statistical and Multivariate Analyses

ANOVA	Analysis of variance
HCPC	Hierarchical clustering on principal components
LSD	Least Significant Difference test (post hoc)

NS	Not significant ($p \geq 0.05$)
p	Probability value (significance thresholds *, **, ***, NS)
PCA	Principal component analysis
r	Pearson correlation coefficient
v-test	Statistic indicating variable contributions in clusters

Units and Derived Quantities

DM	Dry matter (e.g., kg DM kg^{-1} N in NUE units)
g N kg^{-1} DM	Grams of nitrogen per kilogram of dry matter
kg N ha^{-1}	Kilogram of nitrogen per hectare
t ha^{-1}	Tons per hectare

Acknowledgements

This research was conducted as part of the MisTigation project, funded by ADEME (French Environment and Energy Management Agency) through the GRAINE 2022 program. It also benefited from the URGI facilities (https://doi.org/10.15454/1.5572414581735654E12) and was supported by the French government through the National Research Agency (ANR), as part of the France 2030 program for research infrastructure (EQUIPEX+), reference ANR-21-ESRE-0048, as well as Phenome-Emphasis (ANR-11-INBS-0012) and the e-Infrastructure to boost the use of diversified biological resources (reference ANR-22-PEAE-0014). Shehyar Iqbal also received a thesis grant from the Hauts-de-France region and the Biology and Plant Breeding division of INRAE.The authors would like to acknowledge Marie Heumez (GCIE INRAE experimental unit) and all persons who participated in the work.

Funding

This work was supported by Agence de l'Environnement et de la Maîtrise de l'Energie, MisTigation Project 2203D0151.

Conflicts of Interest

The authors declare no conflicts of interest.

Data Availability Statement

The data that support the findings of this study are openly available in Recherche Data Gouv at https://doi.org/10.57745/CEDLW2.

References

Arnoult, S., and M. Brancourt-Hulmel. 2015. "A Review on *Miscanthus* Biomass Production and Composition for Bioenergy Use: Genotypic and Environmental Variability and Implications for Breeding." *Bioenergy Research* 8, no. 2: 502–526. https://doi.org/10.1007/s12155-014-9524-7.

Atienza, S. G., Z. Satovic, K. K. Petersen, O. Dolstra, and A. Martín. 2003. "Identification of QTLs Associated With Yield and Its Components in *Miscanthus sinensis* Anderss." *Euphytica* 132, no. 3: 353–361. https://doi.org/10.1023/A:1025041926259.

Barnaud, C., and R. Muradian. 2024. "Ecosystem Services and Collective Action: New Commons, New Governance Challenges." *Ecosystem Services* 70: 101662. https://doi.org/10.1016/j.ecoser.2024.101662.

Beale, C. V., and S. P. Long. 1997. "Seasonal Dynamics of Nutrient Accumulation and Partitioning in the Perennial C4-Grasses *Miscanthus* × *Giganteus* and *Spartina cynosuroides*." *Biomass and Bioenergy* 12, no. 6: 419–428. https://doi.org/10.1016/S0961-9534(97)00016-0.

Belmokhtar, N., S. Arnoult, B. Chabbert, J.-P. Charpentier, and M. Brancourt-Hulmel. 2017. "Saccharification Performances of *Miscanthus* at the Pilot and Miniaturized Assay Scales: Genotype and Year Variabilities According to the Biomass Composition." *Frontiers in Plant Science* 8: 740. https://doi.org/10.3389/fpls.2017.00740.

Ben Fradj, N., S. Rozakis, M. Borzęcka, and M. Matyka. 2020. "*Miscanthus* in the European Bio-Economy: A Network Analysis." *Industrial Crops and Products* 148: 112281. https://doi.org/10.1016/j.indcrop.2020.112281.

Brancourt-Hulmel, M. 1999. "Crop Diagnosis and Probe Genotypes for Interpreting Genotype Environment Interaction in Winter Wheat Trials." *Theoretical and Applied Genetics* 99: 1018–1030.

Briones, M. J. I., A. Massey, D. M. O. Elias, et al. 2023. "Species Selection Determines Carbon Allocation and Turnover in *Miscanthus* Crops: Implications for Biomass Production and C Sequestration." *Science of the Total Environment* 887: 164003. https://doi.org/10.1016/j.scitotenv.2023.164003.

Byun, C., S. de Blois, and J. Brisson. 2013. "Plant Functional Group Identity and Diversity Determine Biotic Resistance to Invasion by an Exotic Grass." *Journal of Ecology* 101, no. 1: 128–139. https://doi.org/10.1111/1365-2745.12016.

Cadoux, S., F. Ferchaud, C. Demay, et al. 2014. "Implications of Productivity and Nutrient Requirements on Greenhouse Gas Balance of Annual and Perennial Bioenergy Crops." *GCB Bioenergy* 6, no. 4: 425–438. https://doi.org/10.1111/gcbb.12065.

Cadoux, S., A. B. Riche, N. E. Yates, and J.-M. Machet. 2012. "Nutrient Requirements of *Miscanthus* × *Giganteus*: Conclusions From a Review of Published Studies." *Biomass and Bioenergy* 38: 14–22. https://doi.org/10.1016/j.biombioe.2011.01.015.

Chapin, F. S. 1980. "The Mineral Nutrition of Wild Plants." *Annual Review of Ecology and Systematics* 11: 233–260.

Chen, C.-L., H. van der Schoot, S. Dehghan, et al. 2017. "Genetic Diversity of Salt Tolerance in *Miscanthus*." *Frontiers in Plant Science* 8: 187. https://doi.org/10.3389/fpls.2017.00187.

Cibin, R., E. Trybula, I. Chaubey, S. M. Brouder, and J. J. Volenec. 2016. "Watershed-Scale Impacts of Bioenergy Crops on Hydrology and Water Quality Using Improved SWAT Model." *GCB Bioenergy* 8, no. 4: 837–848. https://doi.org/10.1111/gcbb.12307.

Clark, L. V., M. S. Dwiyanti, K. G. Anzoua, et al. 2019. "Genome-Wide Association and Genomic Prediction for Biomass Yield in a Genetically Diverse *Miscanthus sinensis* Germplasm Panel Phenotyped at Five Locations in Asia and North America." *GCB Bioenergy* 11, no. 8: 988–1007. https://doi.org/10.1111/gcbb.12620.

Codina Gironès, V., S. Moret, E. Peduzzi, M. Nasato, and F. Maréchal. 2017. "Optimal Use of Biomass in Large-Scale Energy Systems: Insights for Energy Policy." *Energy* 137: 789–797. https://doi.org/10.1016/j.energy.2017.05.027.

De Vega, J. J., A. Teshome, M. Klaas, J. Grant, J. Finnan, and S. Barth. 2021. "Physiological and Transcriptional Response to Drought Stress Among Bioenergy Grass *Miscanthus* Species." *Biotechnology for Biofuels* 14, no. 1: 60. https://doi.org/10.1186/s13068-021-01915-z.

Dierking, R. M., D. J. Allen, S. M. Brouder, and J. J. Volenec. 2016. "Yield, Biomass Composition, and N Use Efficiency During Establishment of Four *Miscanthus* × *Giganteus* Genotypes as Influenced by N Management." *Biomass and Bioenergy* 91: 98–107. https://doi.org/10.1016/j.biombioe.2016.05.005.

Dierking, R. M., D. J. Allen, S. M. Cunningham, S. M. Brouder, and J. J. Volenec. 2017. "Nitrogen Reserve Pools in Two *Miscanthus* × *Giganteus* Genotypes Under Contrasting N Managements." *Frontiers in Plant Science* 8: 1618. https://doi.org/10.3389/fpls.2017.01618.

Farrell, A. D., J. C. Clifton-Brown, I. Lewandowski, and M. B. Jones. 2006. "Genotypic Variation in Cold Tolerance Influences the Yield of *Miscanthus*." *Annals of Applied Biology* 149, no. 3: 337–345. https://doi.org/10.1111/j.1744-7348.2006.00099.x.

Ferchaud, F., and B. Mary. 2016. "Drainage and Nitrate Leaching Assessed During 7 Years Under Perennial and Annual Bioenergy Crops." *Bioenergy Research* 9, no. 2: 656–670. https://doi.org/10.1007/s12155-015-9710-2.

Ferchaud, F., G. Vitte, J.-M. Machet, N. Beaudoin, M. Catterou, and B. Mary. 2016. "The Fate of Cumulative Applications of 15N-Labelled Fertiliser in Perennial and Annual Bioenergy Crops." *Agriculture, Ecosystems & Environment* 223: 76–86. https://doi.org/10.1016/j.agee.2016.02.030.

Ferrarini, A., F. Fornasier, P. Serra, F. Ferrari, M. Trevisan, and S. Amaducci. 2017. "Impacts of Willow and *Miscanthus* Bioenergy Buffers on Biogeochemical N Removal Processes Along the Soil–Groundwater Continuum." *GCB Bioenergy* 9, no. 1: 246–261. https://doi.org/10.1111/gcbb.12340.

Fry, E. L., S. A. Power, and P. Manning. 2014. "Trait-Based Classification and Manipulation of Plant Functional Groups for Biodiversity–Ecosystem Function Experiments." *Journal of Vegetation Science* 25, no. 1: 248–261. https://doi.org/10.1111/jvs.12068.

Głowacka, K., L. V. Clark, S. Adhikari, et al. 2015. "Genetic Variation in *Miscanthus* × *Giganteus* and the Importance of Estimating Genetic Distance Thresholds for Differentiating Clones." *GCB Bioenergy* 7, no. 2: 386–404. https://doi.org/10.1111/gcbb.12166.

Greef, J. M., M. Deuter, C. Jung, and J. Schondelmaier. 1997. "Genetic Diversity of European *Miscanthus* Species Revealed by AFLP Fingerprinting." *Genetic Resources and Crop Evolution* 44, no. 2: 185–195. https://doi.org/10.1023/A:1008693214629.

Heaton, E. A., F. G. Dohleman, A. F. Miguez, et al. 2010. "Chapter 3–*Miscanthus*: A Promising Biomass Crop." In *Advances in Botanical Research*, edited by J.-C. Kader and M. Delseny, vol. 56, 75–137. Academic Press. https://doi.org/10.1016/B978-0-12-381518-7.00003-0.

Heckman, R., C. Guilherme Pereira, M. Aspinwall, and T. Juenger. 2024. "Physiological Responses of C4 Perennial Bioenergy Grasses to Climate Change: Causes, Consequences, and Constraints." *Annual Review of Plant Biology* 75: 737–769. https://doi.org/10.1146/annurev-arplant-070623-093952.

Hou, W., R. Raverdy, K. Lourgant, et al. 2022. "QTL Detection for Flowering-Time Related Traits in *Miscanthus sinensis* Using a Staggered-Start Design." *Bioenergy Research* 15, no. 2: 718–733. https://doi.org/10.1007/s12155-021-10386-x.

Hromádko, L., V. Vranová, D. Techer, P. Laval-Gilly, K. Rejšek, and P. Formánek. 2010. "Composition of Root Exudates of *Miscanthus* × *Giganteus* Greef et Deu." *Acta Universitatis Agriculturae et Silviculturae Mendelianae Brunensis* 58: 71–76. https://doi.org/10.11118/actaun201058010071.

Husson, F., J. Josse, and J. Pages. 2010. *Principal Component Methods-Hierarchical Clustering-Partitional Clustering: Why Would We Need to Choose for Visualizing Data*, 17. Applied Mathematics Department.

Iqbal, S., M. Brancourt-Hulmel, and M. Zapater. 2025. "Phenotyping Data for 'Nitrogen Economy Strategies Define Distinct Functional Groups of Genotypes in a *Miscanthus sinensis* Progeny'." 10.57745/CEDLW2, Recherche Data Gouv, V1, UNF:6:q03yACXjVm396GREJSrH7g== [fileUNF].

IUSS Working Group WRB. 2022. "World Reference Base for Soil Resources." In *International Soil Classification System for Naming Soils and Creating Legends for Soil Maps*, 4th ed. International Union of Soil Sciences (IUSS).

Justes, E., B. Mary, J.-M. Meynard, J.-M. Machet, and L. Thelier-Huché. 1994. "Determination of a Critical Nitrogen Dilution Curve for Winter Wheat Crops." *Annals of Botany* 74, no. 4: 397–407.

Kumari, A., J. N. Njuguna, X. Zheng, J. Kromdijk, E. J. Sacks, and K. Glowacka. 2024. "Genetic Basis of Non-Photochemical Quenching and Photosystem II Efficiency Responses to Chilling in the Biomass Crop *Miscanthus*." *GCB Bioenergy* 17, no. 1: e70015. https://doi.org/10.1111/gcbb.70015.

Lenhart, K., T. Behrendt, S. Greiner, et al. 2019. "Nitrous Oxide Effluxes From Plants as a Potentially Important Source to the Atmosphere." *New Phytologist* 221, no. 3: 1398–1408. https://doi.org/10.1111/nph.15455.

Leroy, J. 2021. *Etude écophysiologique temporelle dela gestion des réserves carbonées et azotées par trois génotypes de miscanthus*. PhD thesis., 183. AgroParisTech. https://pastel.hal.science/tel-04223136v1.

Leroy, J., F. Ferchaud, C. Giauffret, et al. 2022. "*Miscanthus Sinensis* Is as Efficient as *Miscanthus*×*Giganteus* for Nitrogen Recycling in Spite of Smaller Nitrogen Fluxes." *Bioenergy Research* 15, no. 2: 686–702. https://doi.org/10.1007/s12155-022-10408-2.

Lesur, C., M. Bazot, F. Bio-Beri, B. Mary, M.-H. Jeuffroy, and C. Loyce. 2014. "Assessing Nitrate Leaching During the Three-First Years of *Miscanthus* × *Giganteus* From On-Farm Measurements and Modeling." *GCB Bioenergy* 6, no. 4: 439–449. https://doi.org/10.1111/gcbb.12066.

Lewin, E., J. Clifton Brown, E. Magenau, et al. 2024. "Yield Development and Nutrient Offtake in Contrasting *Miscanthus* Hybrids Under Green and Brown Harvest Regimes." *GCB Bioenergy* 16, no. 8: e13149. https://doi.org/10.1111/gcbb.13149.

Magenau, E., J. Clifton-Brown, D. Awty-Carroll, et al. 2022. "Site Impacts Nutrient Translocation Efficiency in Intraspecies and Interspecies *Miscanthus* Hybrids on Marginal Lands." *GCB Bioenergy* 14, no. 9: 1035–1054. https://doi.org/10.1111/gcbb.12985.

Muhammad, S., B. L. Sanden, B. D. Lampinen, et al. 2020. "Nutrient Storage in the Perennial Organs of Deciduous Trees and Remobilization in Spring—A Study in Almond (*Prunus dulcis*) (Mill.) D. A. Webb." *Frontiers in Plant Science* 11: 658. https://doi.org/10.3389/fpls.2020.00658.

Namoi, N., C. Jang, G. D. Behnke, J. W. Lee, W. Yang, and D. Lee. 2024. "Nitrogen Fertilization Effects on Aged *Miscanthus* × *Giganteus* Stands: Exploring Biomass Yield, Yield Components, and Biomass Prediction Using In-Season Morphological Traits." *GCB Bioenergy* 16, no. 5: e13139. https://doi.org/10.1111/gcbb.13139.

Neukirchen, D., M. Himken, J. Lammel, U. Czypionka-Krause, and H. W. Olfs. 1999. "Spatial and Temporal Distribution of the Root System and Root Nutrient Content of an Established *Miscanthus* Crop." *European Journal of Agronomy* 11, no. 3: 301–309. https://doi.org/10.1016/S1161-0301(99)00031-3.

Nie, G., L. Huang, X. Ma, et al. 2017. "Enriching Genomic Resources and Transcriptional Profile Analysis of *Miscanthus sinensis* Under Drought Stress Based on RNA Sequencing." *International Journal of Genomics* 2017, no. 1: 9184731. https://doi.org/10.1155/2017/9184731.

Nsanganwimana, F., K. S. Al Souki, C. Waterlot, et al. 2021. "Potentials of *Miscanthus* × *Giganteus* for Phytostabilization of Trace Element-Contaminated Soils: Ex Situ Experiment." *Ecotoxicology and Environmental Safety* 214: 112125. https://doi.org/10.1016/j.ecoenv.2021.112125.

Nsanganwimana, F., B. Pourrut, M. Mench, and F. Douay. 2014. "Suitability of *Miscanthus* Species for Managing Inorganic and Organic Contaminated Land and Restoring Ecosystem Services. A Review." *Journal of Environmental Management* 143: 123–134. https://doi.org/10.1016/j.jenvman.2014.04.027.

Olson, S. N., K. Ritter, J. Medley, T. Wilson, W. L. Rooney, and J. E. Mullet. 2013. "Energy Sorghum Hybrids: Functional Dynamics of High Nitrogen Use Efficiency." *Biomass and Bioenergy* 56: 307–316. https://doi.org/10.1016/j.biombioe.2013.04.028.

Pihlatie, M., P. Ambus, J. Rinne, K. Pilegaard, and T. Vesala. 2005. "Plant-Mediated Nitrous Oxide Emissions From Beech (*Fagus sylvatica*) Leaves." *New Phytologist* 168, no. 1: 93–98. https://doi.org/10.1111/j.1469-8137.2005.01542.x.

Ra, K., F. Shiotsu, J. Abe, and S. Morita. 2012. "Biomass Yield and Nitrogen Use Efficiency of Cellulosic Energy Crops for Ethanol Production." *Biomass and Bioenergy* 37: 330–334. https://doi.org/10.1016/j.biombioe.2011.12.047.

Schjoerring, J. K., and M. Mattsson. 2001. "Quantification of Ammonia Exchange Between Agricultural Cropland and the Atmosphere: Measurements Over Two Complete Growth Cycles of Oilseed Rape, Wheat, Barley and Pea." *Plant and Soil* 228, no. 1: 105–115. https://doi.org/10.1023/A:1004851001342.

Scordia, D., E. G. Papazoglou, D. Kotoula, et al. 2022. "Towards Identifying Industrial Crop Types and Associated Agronomies to Improve Biomass Production From Marginal Lands in Europe." *GCB Bioenergy* 14, no. 7: 710–734. https://doi.org/10.1111/gcbb.12935.

Smith, L. C. 2017. *Nitrogen Conservation in Perennial Grasses Managed for Bioenergy Production*. University of Wisconsin-Madison.

Stavridou, E., R. J. Webster, and P. R. H. Robson. 2019. "Novel *Miscanthus* Genotypes Selected for Different Drought Tolerance Phenotypes Show Enhanced Tolerance Across Combinations of Salinity and Drought Treatments." *Annals of Botany* 124, no. 4: 653–674. https://doi.org/10.1093/aob/mcz009.

Steinbach, D., M. Alaux, J. Amselem, et al. 2013. "GnpIS: An Information System to Integrate Genetic and Genomic Data From Plants and Fungi." *Database* 2013: 1–9. https://doi.org/10.1093/database/bat058.

Strullu, L., S. Cadoux, M. Preudhomme, M. H. Jeuffroy, and N. Beaudoin. 2011. "Biomass Production and Nitrogen Accumulation and Remobilisation by *Miscanthus*×*Giganteus* as Influenced by Nitrogen Stocks in Belowground Organs." *Field Crops Research* 121, no. 3: 381–391. https://doi.org/10.1016/j.fcr.2011.01.005.

Sun, Q., Q. Lin, Z.-L. Yi, Z.-R. Yang, and F.-S. Zhou. 2010. "A Taxonomic Revision of *Miscanthus* s.l. (Poaceae) From China." *Botanical Journal of the Linnean Society* 164, no. 2: 178–220. https://doi.org/10.1111/j.1095-8339.2010.01082.x.

Tavakoli-Hashjini, E., A. Piorr, K. Müller, and J. L. Vicente-Vicente. 2020. "Potential Bioenergy Production From *Miscanthus* × *Giganteus* in Brandenburg: Producing Bioenergy and Fostering Other Ecosystem Services While Ensuring Food Self-Sufficiency in the Berlin-Brandenburg Region." *Sustainability* 12, no. 18: 7731. https://www.mdpi.com/2071-1050/12/18/7731.

van der Cruijsen, K., M. Al Hassan, G. van Erven, et al. 2024. "Salt Stress Alters the Cell Wall Components and Structure in *Miscanthus sinensis* Stems." *Physiologia Plantarum* 176, no. 4: e14430. https://doi.org/10.1111/ppl.14430.

van der Weijde, T., L. M. Huxley, S. Hawkins, et al. 2017. "Impact of Drought Stress on Growth and Quality of *Miscanthus* for Biofuel Production." *GCB Bioenergy* 9, no. 4: 770–782. https://doi.org/10.1111/gcbb.12382.

Weik, J., J. Lask, E. Petig, et al. 2022. "Implications of Large-Scale *Miscanthus* Cultivation in Water Protection Areas: A Life Cycle Assessment With Model Coupling for Improved Policy Support." *GCB Bioenergy* 14, no. 11: 1162–1182. https://doi.org/10.1111/gcbb.12994.

Weng, T.-Y., T. Nakashima, A. Villanueva-Morales, J. R. Stewart, E. J. Sacks, and T. Yamada. 2022. "Assessment of Drought Tolerance of *Miscanthus* Genotypes Through Dry-Down Treatment and Fixed-Soil-Moisture-Content Techniques." *Agriculture* 12, no. 1: 6. https://www.mdpi.com/2077-0472/12/1/6.

Wichern, F., E. Eberhardt, J. Mayer, R. G. Joergensen, and T. Müller. 2008. "Nitrogen Rhizodeposition in Agricultural Crops: Methods, Estimates and Future Prospects." *Soil Biology and Biochemistry* 40, no. 1: 30–48. https://doi.org/10.1016/j.soilbio.2007.08.010.

Zapater, M., M. Catterou, B. Mary, et al. 2017. "A Single and Robust Critical Nitrogen Dilution Curve for *Miscanthus* × *Giganteus* and *Miscanthus sinensis*." *Bioenergy Research* 10, no. 1: 115–128. https://doi.org/10.1007/s12155-016-9781-8.

Zhao, H., B. Wang, J. He, et al. 2013. "Genetic Diversity and Population Structure of *Miscanthus sinensis* Germplasm in China." *PLoS One* 8, no. 10: e75672. https://doi.org/10.1371/journal.pone.0075672.

Zheng, C., Z. Yi, L. Xiao, et al. 2022. "The Performance of *Miscanthus* Hybrids in Saline-Alkaline Soil." *Frontiers in Plant Science* 13: 921824. https://doi.org/10.3389/fpls.2022.921824.

Zub, H. W., S. Arnoult, J. Younous, I. Lejeune-Hénaut, and M. Brancourt-Hulmel. 2012. "The Frost Tolerance of *Miscanthus* at the Juvenile Stage: Differences Between Clones Are Influenced by Leaf-Stage and Acclimation." *European Journal of Agronomy* 36, no. 1: 32–40. https://doi.org/10.1016/j.eja.2011.08.001.